DOI: 10.26565/2312-4334-2026-3-14 ISSN 2312-4334

OPTICAL SOLITONS FOR THE CONCATENATION MODEL WITH DIFFERENTIAL GROUP DELAY BY LIE SYMMETRY AND KUMAR-MALIK APPROACH

Rajveer Singhay[1], **Sachin Kumar**[1], **Mohamed E. M. Alngar**[2], **Reham M. A. Shohib**[3], **Lina S. Calucag**[4], **Anjan Biswas**[5,6,7,8,9*]

[1]*Department of Mathematics and Statistics, Central University of Punjab, Bathinda, 151401, Punjab, India*

[2]*Mathematics Education Program, Faculty of Education and Arts, Sohar University, Sohar 311, Oman*

[3]*Basic Science Department, Faculty of Economics and Business Administration, Innovation University, Sharqia, Egypt*

[4]*Department of Mathematics and Science, University of Technology Bahrain, Kingdom of Bahrain*

[5]*Department of Mathematics and Physics, Grambling State University, Grambling, LA–71245, USA*

[6]*Department of Mathematics, Faculty of Science, Karadeniz Technical University, Trabzon—61080, Türkiye*

[7]*Department of Physics and Electronics, Khazar University, Baku, AZ—1096, Azerbaijan*

[8]*Department of Mathematics and Applied Mathematics, Sefako Makgatho Health Sciences University, Medunsa—0204, Pretoria, South Africa*

[9]*Applied Science Research Center, Applied Science Private University, Amman—11937, Jordan*

[*]*Corresponding Author e-mail: biswas.anjan@gmail.com*

Received March 27, 2026; revised August 15, 2026; accepted August 23, 2026

This work examines a generalized concatenation model for birefringent optical fibers and obtains new exact soliton solutions. Using Lie symmetry analysis, the coupled evolution equations are transformed through suitable similarity variables into a manageable system of ordinary differential equations. The resulting reduced system is then treated with the Kumar–Malik method to derive multiple classes of explicit solutions written in Jacobi elliptic, bright soliton, dark soliton, and trigonometric solutions. With appropriate parameter restrictions, these classes simplify to the familiar bright, dark, and periodic soliton waves. To illustrate the physical behavior of the derived structures, representative plots are presented that highlight their propagation features and qualitative stability. Overall, combining symmetry reduction with the Kumar–Malik scheme expands the catalogue of analytical solutions for the concatenation model and deepens understanding of nonlinear pulse dynamics in birefringent media.

Keywords: *Concatenation framework; Lie group symmetry analysis; Kumar–Malik technique; Optical soliton waves; Birefringent fiber media; Jacobi elliptic function solutions*

1. INTRODUCTION

Nonlinear pulse propagation in optical fibers remains a cornerstone of modern nonlinear optics and mathematical physics, particularly in parameter regimes where dispersion, birefringence, and nonlinearity cooperate to generate persistent coherent structures such as solitons, breathers, and rogue waves. With the advent of ultrashort-pulse sources and broadband transmission, higher-order dispersive and nonlinear effects become non-negligible, which naturally motivates the analysis of generalized Schrödinger-type evolution equations and their solution families.

At the modeling level, the nonlinear Schrödinger equation (NLSE) provides a canonical framework for describing envelope dynamics in weakly nonlinear dispersive media, and continues to be refined and applied in diverse optical settings [3, 4]. Beyond the standard NLSE, integrable higher-order extensions have been intensively studied because they preserve analytical tractability while capturing additional physical mechanisms. In this direction, Ankiewicz and Akhmediev presented a higher-order integrable evolution equation together with its soliton solutions, illustrating how higher-order corrections alter waveform characteristics without destroying integrability [1]. Closely related extended NLSE models that include higher-order odd and even terms were further shown to admit extreme localized events, including rogue-wave solutions [2]. Moreover, the integrable quintic nonlinear Schrödinger hierarchy enriches the nonlinear landscape through quintic contributions: soliton solutions were constructed in [9], while breather-to-soliton conversions and breather interactions were investigated in [10, 11]. Collectively, these developments emphasize that higher-order and quintic terms are

Cite as: R. Singhay, S. Kumar, M.E.M. Alngar, R.M.A. Shohib, L.S. Calucag, A. Biswas, East Eur. J. Phys. 3, 160 (2026), https://doi.org/10.26565/2312-4334-2026-3-14

not merely small perturbations; rather, they can substantially broaden the admissible classes of localized structures and transition scenarios.

Another important strand of research concerns unified descriptions that connect several prominent Schrödinger-type equations within a single formalism. In particular, concatenation-type models provide a coupled framework that can incorporate higher-order dispersion and nonlinear corrections systematically, while linking to celebrated integrable equations such as the NLSE [3, 4], the Lakshmanan–Porsezian–Daniel (LPD) equation [5, 6], and the Sasa–Satsuma equation (SSE) [7, 8]. Recent studies have also highlighted the relevance of concatenation settings for realistic birefringent configurations by incorporating differential group delay and constructing corresponding optical soliton solutions [12, 13]. Despite the growing literature, explicit closed-form solutions remain of continuing value: they provide benchmarks for numerical algorithms, enable parametric studies of waveform switching (e.g., bright versus dark profiles), and clarify how higher-order coefficients shape pulse evolution.

Motivated by these considerations, the present work investigates the coupled concatenation system (Eqs. (1)–(2)) for the complex envelopes $q(x,t)$ and $r(x,t)$, which represent two orthogonally polarized field components. By exploiting Lie symmetries, we determine appropriate invariants that transform the governing PDE system into an equivalent ODE system. The reduced equations are then solved exactly using the Kumar–Malik technique. The resulting waveforms are expressed in Jacobi elliptic, hyperbolic, and trigonometric forms and, under suitable parameter constraints, yield bright-, dark-, and periodic-soliton profiles. Finally, representative plots are provided to illustrate characteristic propagation features and to demonstrate the influence of key physical and model parameters.

1.1. Governing Model

In this study, we consider the following coupled concatenation model [12, 13]:

$$
\begin{aligned}
&iq_t + a_1 q_{xx} + \left(b_1|q|^2 + c_1|r|^2\right)q + c_{11}\Big[\sigma_{11}q_{xxxx} + \{\alpha_1(q_x)^2 + \mathfrak{w}_1(r_x)^2\}q^* \\
&\quad + (\gamma_1|q_x|^2 + \lambda_1|r_x|^2)q + (\delta_1|q|^2 + \zeta_1|r|^2)q_{xx} + (\mu_1 q^2 + \rho_1 r^2)q^*_{xx} \\
&\quad + (f_1|q|^4 + g_1|q|^2|r|^2 + h_1|r|^4)q\Big] + ic_{21}\Big[\sigma_{71}q_{xxx} + (\eta_1|q|^2 + \theta_1|r|^2)q_x \\
&\quad + (\varepsilon_1 q^2 + \tau_1 r^2)q^*_x\Big] = 0,
\end{aligned}
\tag{1}
$$

$$
\begin{aligned}
&ir_t + a_2 r_{xx} + \left(b_2|r|^2 + c_2|q|^2\right)r + c_{12}\Big[\sigma_{12}r_{xxxx} + \{\alpha_2(r_x)^2 + \mathfrak{w}_2(q_x)^2\}r^* \\
&\quad + (\gamma_2|r_x|^2 + \lambda_2|q_x|^2)r + (\delta_2|r|^2 + \zeta_2|q|^2)r_{xx} + (\mu_2 r^2 + \rho_2 q^2)r^*_{xx} \\
&\quad + (f_2|r|^4 + g_2|r|^2|q|^2 + h_2|q|^4)r\Big] + ic_{22}\Big[\sigma_{72}r_{xxx} + (\eta_2|r|^2 + \theta_2|q|^2)r_x \\
&\quad + (\varepsilon_2 r^2 + \tau_2 q^2)r^*_x\Big] = 0.
\end{aligned}
\tag{2}
$$

In this system, $q(x,t)$ and $r(x,t)$ represent the complex slowly varying envelopes associated with two mutually orthogonal polarization modes. The coefficients a_1 and a_2 characterize the group-velocity dispersion, while b_j and c_j ($j = 1,2$) measure self-phase modulation and cross-phase modulation, respectively. The set of parameters σ, α, $\mathfrak{w}$, γ, λ, δ, ζ, μ, ρ, f, g, and h models higher-order mechanisms such as nonlinear dispersion, self-frequency shifting, and fourth-order corrections. Hence, the coupled system captures the dynamics of birefringent optical pulses influenced by cubic–quartic nonlinearities together with third- and fourth-order dispersion.

In this study, we employ Lie symmetry analysis for the concatenation model (1)–(2). The admitted symmetries provide suitable similarity transformations that reduce the coupled PDE system to a tractable set of ordinary differential equations. The reduced system is then treated analytically via the Kumar–Malik method, leading to several new classes of exact solutions in Jacobi elliptic, hyperbolic, and trigonometric forms. For appropriate choices of the governing parameters, these solution families recover the familiar bright-, dark-, and periodic-soliton profiles reported in the literature.

Graphical illustrations are presented to highlight the propagation features of the derived solutions and to explore the impact of the physical parameters on soliton amplitude, width, and robustness. These findings broaden the available catalogue of analytical solutions for the concatenation model and offer further insight into nonlinear pulse evolution in birefringent optical fibers.

The remainder of this paper is organized as follows. In Section 2, we perform the Lie symmetry analysis of the model and determine the associated infinitesimal generators. Section 3 is devoted to the similarity reductions that convert the governing PDE system into a reduced set of ODEs. In Section 4, the Kumar–Malik method is implemented to obtain exact analytical soliton solutions. Section 5 presents representative plots and discusses their physical implications. Finally, Section 6 summarizes the main findings and outlines possible directions for future work.

2. LIE SYMMETRY ANALYSIS

The Lie symmetry approach [14] provides a systematic framework for reducing nonlinear partial differential equations to ordinary differential equations by exploiting their admitted continuous symmetry groups. After determining the infinitesimal symmetry generators, one constructs the associated invariants (similarity variables), which transform the original PDE into a reduced equation of lower dimensionality. In the present work, this methodology is applied to the concatenation model (1) to derive its symmetry algebra and to obtain the corresponding similarity reductions.

Next, we introduce the real-valued decompositions

$$q(t,x) = u_1(t,x) + i\, v_1(t,x), \qquad r(t,x) = u_2(t,x) + i\, v_2(t,x),$$

and substitute them into Eq. (1). Separating the resulting expression into its real and imaginary components leads to the following system of partial differential equations:

$$\begin{aligned}
&c_{1l}\,\sigma_{1l}\,(v_l)_{xxxx} + c_{2l}\,\sigma_{7l}\,(u_l)_{xxx} + \Big(c_{1l}(\mu_l+\delta_l)\,v_l^2 - c_{1l}(\mu_l-\delta_l)\,u_l^2 - c_{1l}(\rho_l-\zeta_l)\,u_m^2 \\
&\quad + c_{1l}(\rho_l+\zeta_l)\,v_m^2 + a_l\Big)(v_l)_{xx} + 2c_{1l}\big(\mu_l u_l v_l + \rho_l u_m v_m\big)(u_l)_{xx} - v_l c_{1l}(\alpha_l-\gamma_l)(u_{l,x})^2 \\
&\quad + \Big(2c_{1l}\alpha_l(v_{l,x})u_l + c_{2l}\big((\eta_l-\varepsilon_l)v_l^2 + (\eta_l+\varepsilon_l)u_l^2 + (\tau_l+\theta_l)u_m^2 - v_m^2(\tau_l-\theta_l)\big)\Big)(u_{l,x}) \\
&\quad + v_l c_{1l}(\alpha_l+\gamma_l)(v_{l,x})^2 + 2c_{2l}\big(\tau_l u_m v_m + \varepsilon_l u_l v_l\big)(v_{l,x}) - v_l c_{1l}(\mathfrak{w}_l-\lambda_l)(u_{m,x})^2 \\
&\quad + 2c_{1l}\mathfrak{w}_l(u_{m,x})(v_{m,x})u_l + v_l c_{1l}(\mathfrak{w}_l+\lambda_l)(v_{m,x})^2 + u_{l,t} \\
&\quad + c_{1l} f_l v_l^5 + \big(2f_l c_{1l}u_l^2 + g_l c_{1l}u_m^2 + g_l c_{1l}v_m^2 + b_l\big)v_l^3 \\
&\quad + \Big(f_l c_{1l}u_l^4 + (g_l c_{1l}u_m^2 + g_l c_{1l}v_m^2 + b_l)u_l^2 + h_l c_{1l}u_m^4 + (2h_l c_{1l}v_m^2 + c_l)u_m^2 + h_l c_{1l}v_m^4 + c_l v_m^2\Big)v_l = 0, \\
&c_{1l}\,\sigma_{1l}\,(u_l)_{xxxx} - c_{2l}\,\sigma_{7l}\,(v_l)_{xxx} + \Big(c_{1l}(\mu_l+\delta_l)\,u_l^2 - c_{1l}(\mu_l-\delta_l)\,v_l^2 + c_{1l}(\rho_l+\zeta_l)\,u_m^2 \\
&\quad - c_{1l}(\rho_l-\zeta_l)\,v_m^2 + a_l\Big)(u_l)_{xx} + 2c_{1l}\big(\mu_l u_l v_l + \rho_l u_m v_m\big)(v_l)_{xx} - u_l c_{1l}(\alpha_l-\gamma_l)(v_{l,x})^2 \\
&\quad + \Big(2c_{1l}\alpha_l(u_{l,x})v_l - c_{2l}\big((\eta_l-\varepsilon_l)u_l^2 + (\eta_l+\varepsilon_l)v_l^2 + (-\tau_l+\theta_l)u_m^2 + v_m^2(\tau_l+\theta_l)\big)\Big)(v_{l,x}) \\
&\quad + u_l c_{1l}(\alpha_l+\gamma_l)(u_{l,x})^2 - 2c_{2l}\big(\tau_l u_m v_m + \varepsilon_l u_l v_l\big)(u_{l,x}) \\
&\quad + u_l c_{1l}(\mathfrak{w}_l+\lambda_l)(u_{m,x})^2 + 2c_{1l}\mathfrak{w}_l(u_{m,x})(v_{m,x})v_l - u_l c_{1l}(\mathfrak{w}_l-\lambda_l)(v_{m,x})^2 - v_{l,t} \\
&\quad + c_{1l} f_l u_l^5 + \big(g_l c_{1l}u_m^2 + 2f_l c_{1l}v_l^2 + g_l c_{1l}v_m^2 + b_l\big)u_l^3 \\
&\quad + \Big(f_l c_{1l}v_l^4 + (g_l c_{1l}u_m^2 + g_l c_{1l}v_m^2 + b_l)v_l^2 + h_l c_{1l}u_m^4 + (2h_l c_{1l}v_m^2 + c_l)u_m^2 + h_l c_{1l}v_m^4 + c_l v_m^2\Big)u_l = 0,
\end{aligned} \tag{3}$$

where $l \in \{1,2\}$ and $m = 3 - l$ denotes the complementary index.

Next, we introduce a one-parameter Lie group of infinitesimal transformations defined by:

$$\begin{aligned}
x^* &= x + \epsilon\chi(x,t,u_1,v_1,u_2,v_2) + O(\epsilon^2), \\
t^* &= t + \epsilon\Theta(x,t,u_1,v_1,u_2,v_2) + O(\epsilon^2), \\
{u_1}^* &= u_1 + \epsilon\Psi_1(x,t,u_1,v_1,u_2,v_2) + O(\epsilon^2), \\
{v_1}^* &= v_1 + \epsilon\Phi_1(x,t,u_1,v_1,u_2,v_2) + O(\epsilon^2), \qquad (4) \\
{u_2}^* &= u_2 + \epsilon\Psi_2(x,t,u_1,v_1,u_2,v_2) + O(\epsilon^2), \\
{v_2}^* &= v_2 + \epsilon\Phi_2(x,t,u_1,v_1,u_2,v_2) + O(\epsilon^2), \qquad (5)
\end{aligned}$$

Here, χ, Θ, Ψ_1, Φ_1, Ψ_2, and Φ_2 denote the infinitesimal generator components associated with the variables x, t, u_1, v_1, u_2, and v_2, respectively, and $\epsilon \in \mathbb{R}$ is the group parameter. These transformations are required to leave Eq. (3) invariant under the induced Lie-group action.

The corresponding infinitesimal vector field is given by:

$$X = \chi\frac{\partial}{\partial x} + \Theta\frac{\partial}{\partial t} + \sum_{l=1}^{2}\left(\Psi_l\frac{\partial}{\partial u_l} + \Phi_l\frac{\partial}{\partial v_l}\right). \tag{6}$$

To compute the admitted symmetries, we impose the standard invariance condition:

$$\mathrm{pr}^{(4)}(X)(\Delta)\big|_{\Delta=0} = 0, \tag{7}$$

where $\mathrm{pr}^{(4)}X$ denotes the fourth-order prolongation of the vector field X, defined by:

$$\begin{aligned}\mathrm{pr}^{(4)}X =& X + \sum_{l=1}^{2}\left(\Psi_l^t\frac{\partial}{\partial u_{l,t}} + \Psi_l^x\frac{\partial}{\partial u_{l,x}} + \Psi_l^{xx}\frac{\partial}{\partial u_{l,xx}} + \Psi_l^{xxx}\frac{\partial}{\partial u_{l,xxx}} + \Psi_l^{xxxx}\frac{\partial}{\partial u_{l,xxxx}}\right)\\ &+ \sum_{l=1}^{2}\left(\Phi_l^t\frac{\partial}{\partial v_{l,t}} + \Phi_l^x\frac{\partial}{\partial v_{l,x}} + \Phi_l^{xx}\frac{\partial}{\partial v_{l,xx}} + \Phi_l^{xxx}\frac{\partial}{\partial v_{l,xxx}} + \Phi_l^{xxxx}\frac{\partial}{\partial v_{l,xxxx}}\right).\end{aligned}$$

The coefficients of the prolonged vector field are evaluated using the total derivative operators:

$$\begin{aligned}
\Psi_l^t &= D_t(\Psi_l) - D_t(\chi)\,u_{l,x} - D_t(\Theta)\,u_{l,t},\\
\Phi_l^t &= D_t(\Phi_l) - D_t(\chi)\,v_{l,x} - D_t(\Theta)\,v_{l,t},\\
\Psi_l^x &= D_x(\Psi_l) - D_x(\chi)\,u_{l,x} - D_x(\Theta)\,u_{l,t},\\
\Phi_l^x &= D_x(\Phi_l) - D_x(\chi)\,v_{l,x} - D_x(\Theta)\,v_{l,t},\\
\Psi_l^{xx} &= D_x(\Psi_l^x) - D_x(\chi)\,u_{l,xx} - D_x(\Theta)\,u_{l,xt},\\
\Phi_l^{xx} &= D_x(\Phi_l^x) - D_x(\chi)\,v_{l,xx} - D_x(\Theta)\,v_{l,xt},\\
\Psi_l^{xxx} &= D_x(\Psi_l^{xx}) - D_x(\chi)\,u_{l,xxx} - D_x(\Theta)\,u_{l,xxt},\\
\Phi_l^{xxx} &= D_x(\Phi_l^{xx}) - D_x(\chi)\,v_{l,xxx} - D_x(\Theta)\,v_{l,xxt},\\
\Psi_l^{xxxx} &= D_x(\Psi_l^{xxx}) - D_x(\chi)\,u_{l,xxxx} - D_x(\Theta)\,u_{l,xxxt},\\
\Phi_l^{xxxx} &= D_x(\Phi_l^{xxx}) - D_x(\chi)\,v_{l,xxxx} - D_x(\Theta)\,v_{l,xxxt},
\end{aligned}$$

Here, D_x and D_t are the total-derivative operators with respect to x and t, respectively, as described in [15]. Applying the invariance condition (7) to Eq. (3) yields:

$$
\begin{aligned}
&\Big(\big((\mu_l+\delta_l)\,v_l^2+(-\mu_l+\delta_l)\,u_l^2+(-\rho_l+\zeta_l)\,u_m^2+(\rho_l+\zeta_l)\,v_m^2\big)\,c_{1l}+a_l\Big)\,\Phi_l^{\{xx\}}+2\,\Psi_l^{\{xx\}}\,c_{1l}\,(\mu_l u_l v_l+\rho_l u_m v_m)\\
&\quad+\Phi_l^{\{xxxx\}}\,c_{1l}\,\sigma_{1l}+\Psi_l^{\{xxx\}}\,c_{2l}\,\sigma_{7l}+\Big(\big(-2\,u_{l,x}(\alpha_l-\gamma_l)\,v_l+2\,v_{l,x}\alpha_l\,u_l\big)\,c_{1l}+c_{2l}\big((\eta_l-\varepsilon_l)v_l^2+(\eta_l+\varepsilon_l)u_l^2\\
&\quad+(\tau_l+\theta_l)u_m^2-(\tau_l-\theta_l)v_m^2\big)\Big)\,\Psi_l^x+\Big(\big(2\,v_{l,x}(\alpha_l+\gamma_l)\,v_l+2\,u_{l,x}\alpha_l\,u_l\big)\,c_{1l}+2\,c_{2l}(\tau_l u_m v_m+\varepsilon_l u_l v_l)\Big)\,\Phi_l^x\\
&\quad+2\big(v_{m,x}(\mathfrak{w}_l+\lambda_l)\,v_l+u_{m,x}\mathfrak{w}_l\,u_l\big)\,c_{1l}\,\Phi_m^x-2\big(u_{m,x}(\mathfrak{w}_l-\lambda_l)\,v_l-v_{m,x}\mathfrak{w}_l\,u_l\big)\,c_{1l}\,\Psi_m^x+\Psi_l^t\\
&\quad+\Big(5\,\Phi_l\,f_l\,v_l^4+\big(2\Phi_m\,g_l\,v_m+4\Psi_l\,f_l\,u_l+2\Psi_m\,g_l\,u_m\big)\,v_l^3+\big(6f_l\,u_l^2+3g_l\,u_m^2+3g_l\,v_m^2\big)\,\Phi_l\,v_l^2\\
&\quad+\Big((2\mu_l+2\delta_l)\,v_{l,xx}\,\Phi_l+4\Psi_l\,f_l\,u_l^3+(2\Phi_m\,g_l\,v_m+2\Psi_m\,g_l\,u_m)\,u_l^2+(2\Psi_l\,g_l\,u_m^2+2\Psi_l\,g_l\,v_m^2)\,u_l\\
&\quad+4\Psi_m\,h_l\,u_m^3+4\Phi_m\,h_l\,u_m^2 v_m+4\Psi_m\,h_l\,u_m v_m^2+4\Phi_m\,h_l\,v_m^3+2\Psi_l\,\mu_l\,u_{l,xx}\Big)\,v_l+\Big(f_l\,u_l^4+(g_l\,u_m^2+g_l\,v_m^2)\,u_l^2\\
&\quad+2\mu_l u_l\,u_{l,xx}+h_l\,u_m^4+2h_l u_m^2 v_m^2+h_l v_m^4+(-\alpha_l+\gamma_l)\,u_{l,x}^2+(\alpha_l+\gamma_l)\,v_{l,x}^2+(-u_{m,x}^2+v_{m,x}^2)\mathfrak{w}_l+u_{m,x}^2\lambda_l\\
&\quad+v_{m,x}^2\lambda_l\Big)\,\Phi_l+(-2\mu_l+2\delta_l)\,v_{l,xx}\,\Psi_l\,u_l+\big(2\rho_l\,u_{l,xx}\,\Phi_m+(-2\rho_l+2\zeta_l)\,v_{l,xx}\,\Psi_m\big)\,u_m\\
&\quad+\big((2\rho_l+2\zeta_l)\,v_{l,xx}\,\Phi_m+2\Psi_m\,\rho_l\,u_{l,xx}\big)\,v_m+2\Psi_l\,\alpha_l\,u_{l,x}v_{l,x}+2\Psi_l\,\mathfrak{w}_l\,u_{m,x}v_{m,x}\Big)\,c_{1l}+3\Phi_l\,b_l\,v_l^2\\
&\quad+\Big((2\eta_l-2\varepsilon_l)\,u_{l,x}\,c_{2l}\,\Phi_l+2c_{2l}\Psi_l\,v_{l,x}\,\varepsilon_l+2\Psi_m\,c_l\,u_m+2\Phi_m\,c_l\,v_m+2\Psi_l\,b_l\,u_l\Big)\,v_l\\
&\quad+\big(2c_{2l}u_l\varepsilon_l v_{l,x}+b_l\,u_l^2+c_l\,u_m^2+c_l\,v_m^2\big)\,\Phi_l+(2\eta_l+2\varepsilon_l)\,\Psi_l\,u_{l,x}\,c_{2l}\,u_l\\
&\quad+\big((2\tau_l+2\theta_l)\Psi_m\,u_{l,x}+2\Phi_m\,\tau_l\,v_{l,x}\big)\,c_{2l}\,u_m+\big((-2\tau_l+2\theta_l)\Phi_m\,u_{l,x}+2\Psi_m\,\tau_l\,v_{l,x}\big)\,c_{2l}\,v_m\ =\ 0,\\
&\Big(\big((\mu_l+\delta_l)\,u_l^2+(-\mu_l+\delta_l)\,v_l^2+(\rho_l+\zeta_l)\,u_m^2-(\rho_l-\zeta_l)\,v_m^2\big)\,c_{1l}+a_l\Big)\,\Psi_l^{\{xx\}}+2\,\Phi_l^{\{xx\}}\,c_{1l}\,(\mu_l u_l v_l+\rho_l u_m v_m)\\
&\quad+\Psi_l^{\{xxxx\}}\,c_{1l}\,\sigma_{1l}-\Phi_l^{\{xxx\}}\,c_{2l}\,\sigma_{7l}+\Big(\big(-2\,v_{l,x}(\alpha_l-\gamma_l)\,u_l+2\,v_l\,u_{l,x}\alpha_l\big)\,c_{1l}+c_{2l}\big((-\eta_l+\varepsilon_l)u_l^2\\
&\quad+(-\eta_l-\varepsilon_l)v_l^2+(\tau_l-\theta_l)u_m^2-(\tau_l+\theta_l)v_m^2\big)\Big)\,\Phi_l^x+\Big(\big(2\,u_{l,x}(\alpha_l+\gamma_l)\,u_l+2\,v_l\,v_{l,x}\alpha_l\big)\,c_{1l}\\
&\quad-2\,c_{2l}(\tau_l u_m v_m+\varepsilon_l u_l v_l)\Big)\,\Psi_l^x+2\big(-v_{m,x}(\mathfrak{w}_l-\lambda_l)\,u_l+v_l\,u_{m,x}\mathfrak{w}_l\big)\,c_{1l}\,\Phi_m^x+2\,c_{1l}\big(u_{m,x}(\mathfrak{w}_l+\lambda_l)\,u_l\\
&\quad+v_l\,v_{m,x}\mathfrak{w}_l\big)\,\Psi_m^x-\Phi_l^t+\Big(5\,\Psi_l\,f_l\,u_l^4+\big(4\Phi_l\,f_l\,v_l+2\Phi_m\,g_l\,v_m+2\Psi_m\,g_l\,u_m\big)\,u_l^3\\
&\quad+\big(6f_l\,v_l^2+3g_l\,u_m^2+3g_l\,v_m^2\big)\,\Psi_l\,u_l^2+\Big((2\mu_l+2\delta_l)\,u_{l,xx}\,\Psi_l+4\Phi_l\,f_l\,v_l^3+(2\Phi_m\,g_l\,v_m+2\Psi_m\,g_l\,u_m)\,v_l^2\\
&\quad+(2\Phi_l\,g_l\,u_m^2+2\Phi_l\,g_l\,v_m^2)\,v_l+4\Psi_m\,h_l\,u_m^3+4\Phi_m\,h_l\,u_m^2 v_m+4\Psi_m\,h_l\,u_m v_m^2+4\Phi_m\,h_l\,v_m^3+2\Phi_l\,\mu_l\,v_{l,xx}\Big)\,u_l\\
&\quad+\Big(f_l\,v_l^4+(g_l\,u_m^2+g_l\,v_m^2)\,v_l^2+2\mu_l v_l\,v_{l,xx}+h_l\,u_m^4+2h_l u_m^2 v_m^2+h_l v_m^4+(-\alpha_l+\gamma_l)\,v_{l,x}^2\\
&\quad+(\alpha_l+\gamma_l)\,u_{l,x}^2+(u_{m,x}^2-v_{m,x}^2)\mathfrak{w}_l+u_{m,x}^2\lambda_l+v_{m,x}^2\lambda_l\Big)\,\Psi_l+(-2\mu_l+2\delta_l)\,u_{l,xx}\,\Phi_l\,v_l\\
&\quad+\big(2\rho_l\,v_{l,xx}\,\Phi_m+(2\rho_l+2\zeta_l)\,u_{l,xx}\,\Psi_m\big)\,u_m+\big((-2\rho_l+2\zeta_l)\,u_{l,xx}\,\Phi_m+2\Psi_m\,\rho_l\,v_{l,xx}\big)\,v_m\\
&\quad+2\Phi_l\,\alpha_l\,u_{l,x}v_{l,x}+2\Phi_l\,\mathfrak{w}_l\,u_{m,x}v_{m,x}\Big)\,c_{1l}+3\Psi_l\,b_l\,u_l^2+\Big((-2\eta_l+2\varepsilon_l)\,v_{l,x}\,c_{2l}\,\Psi_l-2c_{2l}\Phi_l\,u_{l,x}\,\varepsilon_l\\
&\quad+2\Psi_m\,c_l\,u_m+2\Phi_l\,b_l\,v_l+2\Phi_m\,c_l\,v_m\Big)\,u_l+\big(-2c_{2l}v_l\varepsilon_l u_{l,x}+b_l\,v_l^2+c_l\,u_m^2+c_l\,v_m^2\big)\,\Psi_l\\
&\quad+(-2\eta_l-2\varepsilon_l)\,\Phi_l\,v_{l,x}\,c_{2l}\,v_l+\big((2\tau_l-2\theta_l)\Psi_m\,v_{l,x}-2\Phi_m\,\tau_l\,u_{l,x}\big)\,c_{2l}\,u_m+\big((-2\tau_l-2\theta_l)\Phi_m\,v_{l,x}\\
&\quad-2\Psi_m\,\tau_l\,u_{l,x}\big)\,c_{2l}\,v_m\ =\ 0
\end{aligned}
\tag{8}
$$

where $l = 1, 2$ and $m = 3 - l$.

Substituting the expressions for $(\Psi_l^x, \Phi_l^x, \Psi_l^{\{xx\}}, \Phi_l^{\{xx\}}, \Psi_l^t, \Phi_l^t, \ldots)$ into Eq. (8), we obtain the following determining system:

$$
\begin{aligned}
&\Psi_{1t} = 0, \quad \Psi_{1u_1} = 0, \quad \Psi_{1u_2} = 0, \quad \Psi_{1v_1} = \frac{\Psi_1}{v_1}, \quad \Psi_{1v_2} = 0, \quad \Psi_{1x} = 0,\\
&\Theta_t = 0, \quad \Theta_{u_1} = 0, \quad \Theta_{u_2} = 0, \quad \Theta_{v_1} = 0, \quad \Theta_{v_2} = 0, \quad \Theta_x = 0,\\
&\chi_t = 0, \quad \chi_{u_1} = 0, \quad \chi_{u_2} = 0, \quad \chi_{v_1} = 0, \quad \chi_{v_2} = 0, \quad \chi_x = 0,\\
&\Psi_2 = \Psi_1\frac{v_2}{v_1}, \quad \Phi_1 = -\Psi_1\frac{u_1}{v_1}, \quad \Phi_2 = -\Psi_1\frac{u_2}{v_1}.
\end{aligned}
\tag{9}
$$

Throughout, subscripts such as t, x, u_1, u_2, v_1, and v_2 indicate partial differentiation with respect to the corresponding variables; for instance,

$$
\Psi_{1t} = \frac{\partial \Psi_1}{\partial t}.
$$

Solving the determining system (9) yields the following infinitesimal symmetries:

$$
\begin{aligned}
&\Psi_l(x,t,u_1,v_1,u_2,v_2) = C_3\, v_l, \qquad \Phi_l(x,t,u_1,v_1,u_2,v_2) = -C_3\, u_l,\\
&\Theta(x,t,u_1,v_1,u_2,v_2) = C_1, \qquad \chi(x,t,u_1,v_1,u_2,v_2) = C_2,
\end{aligned}
\quad \text{where } l = 1,2.
\tag{10}
$$

Substituting the obtained expressions for χ, Θ, Ψ_l, and Φ_l into the infinitesimal generator produces three basis vector fields that span the symmetry algebra of system (3):

$$
\begin{aligned}
X_1 &= \partial_t,\\
X_2 &= \partial_x,\\
X_3 &= \sum_{l=1}^{2}\Big(v_l\partial_{u_l} - u_l\partial_{v_l}\Big).
\end{aligned}
\tag{11}
$$

3. SYMMETRY REDUCTION

We now perform the symmetry reduction of Eq. (1) associated with the vector field $\varrho_1 X_1 + \varrho_2 X_2 + X_3$, where ϱ_1 and ϱ_2 are arbitrary constants, is obtained from Lagrange's auxiliary equations:

$$
\frac{dt}{\varrho_1} = \frac{dx}{\varrho_2} = \frac{du_1}{v_1} = \frac{dv_1}{-u_1} = \frac{du_2}{v_2} = \frac{dv_2}{-u_2}.
\tag{12}
$$

Solving Eq. (12) gives the similarity variables

$$
\xi = \varrho_1 x - \varrho_2 t, \quad u_l(x,t) = P_l(\xi)\cos Q, \qquad v_l(x,t) = P_l(\xi)\sin Q,
\tag{13}
$$

where $Q = -\kappa x + \omega t + \theta_0$ and $l = 1,2$.
From Eq. (13), we obtain

$$
\begin{aligned}
q(x,t) &= P_1(\xi)e^{iQ},\\
r(x,t) &= P_2(\xi)e^{iQ}.
\end{aligned}
\tag{14}
$$

Substituting the similarity form (14) into Eq. (1) and splitting the result into its real and imaginary components leads to the following reduced system of ordinary differential equations:

for $l = 1, 2,\ m = 3 - l$:

$$\begin{aligned}
&\big(-4\, c_{1l}\, \kappa\, \sigma_{1l} + c_{2l}\, \sigma_{7l} \big)\, \varrho_1^3\, \frac{d^3 P_l}{d\xi^3} + \frac{dP_l}{d\xi} \Bigg\{ \varrho_1 \Big[4\, c_{1l}\, \sigma_{1l}\, \kappa^3 - 3\, c_{2l}\, \sigma_{7l}\, \kappa^2 - 2\, \kappa\, a_l \Big] - \varrho_2 \\
&\quad + \varrho_1 \Big[\big(2\kappa\, c_{1l} (\mu_l - \alpha_l - \delta_l) + c_{2l} (\eta_l + \varepsilon_l) \big)\, P_l(\xi)^2 \Big] + \varrho_1 \Big[\big(2\kappa\, c_{1l} (\rho_l - \zeta_l) + c_{2l} (\tau_l + \theta_l) \big)\, P_m(\xi)^2 \Big] \Bigg\} \\
&\quad - 2\, \mathfrak{w}_l\, c_{1l}\, \kappa\, \varrho_1\, P_l(\xi)\, P_m(\xi)\, \frac{dP_m}{d\xi} \;=\; 0, \\
&c_{1l}\, \varrho_1^4\, \sigma_{1l}\, \frac{d^4 P_l}{d\xi^4} + \Big(-6\, c_{1l}\, \kappa^2\, \sigma_{1l} + 3\, \kappa\, c_{2l}\, \sigma_{7l} + c_{1l} (\mu_l + \delta_l)\, P_l(\xi)^2 + c_{1l} (\rho_l + \zeta_l)\, P_m(\xi)^2 + a_l \Big)\, \varrho_1^2\, \frac{d^2 P_l}{d\xi^2} \\
&+ P_l(\xi) \Big[c_{1l}\, \kappa^4\, \sigma_{1l} - c_{2l}\, \kappa^3\, \sigma_{7l} - \kappa^2 \Big(c_{1l} (\mu_l + \alpha_l + \delta_l - \gamma_l)\, P_l(\xi)^2 + c_{1l} (\rho_l + \zeta_l + \mathfrak{w}_l - \lambda_l)\, P_m(\xi)^2 + a_l \Big) \\
&+ \kappa\, c_{2l} \Big((\eta_l - \varepsilon_l)\, P_l(\xi)^2 - (\tau_l - \theta_l)\, P_m(\xi)^2 \Big) + \big(h_l\, c_{1l}\, P_m(\xi)^4 + c_l\, P_m(\xi)^2 \big) \Big] + P_l(\xi)\, c_{1l} (\alpha_l + \gamma_l) \left(\frac{dP_l}{d\xi} \right)^2 \varrho_1^2 \\
&+\ c_{1l} \varrho_1^2 (\mathfrak{w}_l + \lambda_l) P_l(\xi) \left(\frac{dP_m}{d\xi} \right)^2 - \omega\, P_l(\xi) + c_{1l}\, f_l\, P_l(\xi)^5 + \big(g_l\, c_{1l}\, P_m(\xi)^2 + b_l \big)\, P_l(\xi)^3 = 0.
\end{aligned} \tag{15}$$

Taking the soliton speed ϱ_2 as

$$\varrho_2 = 4\, c_{1l}\, \kappa^3\, \sigma_{1l}\, \varrho_1 - 3\, c_{2l}\, \kappa^2\, \sigma_{7l}\, \varrho_1 - 2\, a_l\, \kappa\, \varrho_1, \qquad l = 1, 2. \tag{16}$$

Under the following parametric restrictions

$$\begin{aligned}
&2\, c_{1l}\, (\rho_l - \zeta_l)\, \varrho_1\, \kappa + c_{2l}\, (\tau_l + \theta_l)\, \varrho_1 = 0, \\
&2\, (\mu_l - \alpha_l - \delta_l)\, c_{1l}\, \varrho_1\, \kappa + c_{2l}\, (\eta_l + \varepsilon_l)\, \varrho_1 = 0, \\
&-4\, c_{1l}\, \kappa\, \sigma_{1l} + c_{2l}\, \sigma_{7l} = 0, \\
&\mathfrak{w}_l = 0, \qquad l = 1, 2.
\end{aligned} \tag{17}$$

Moreover, equating the two expressions for the wave speed and using the above parameter constraints yields

$$\begin{aligned}
&a_1 = a_2 = a, \qquad c_{21} = c_{22} = c_7, \qquad \sigma_{71} = \sigma_{72} = \sigma_7, \\
&\zeta_l = 2\, \sigma_{1l}\, \frac{(\tau_l + \theta_l)}{\sigma_7} + \rho_l, \qquad l = 1, 2, \\
&\eta_l = \frac{(-\mu_l + \alpha_l + \delta_l)\, \sigma_7}{2\, \sigma_{1l}} - \varepsilon_l, \qquad l = 1, 2, \\
&c_{11} = c_{12}\, \frac{\sigma_{12}}{\sigma_{11}}, \qquad c_7 = \frac{4\, c_{12}\, \kappa\, \sigma_{12}}{\sigma_7}.
\end{aligned} \tag{18}$$

Consequently, the wave speed can be expressed in the equivalent form

$$\varrho_2 = -2\, \kappa\, \varrho_1\, \big(c_7\, \kappa\, \sigma_7 + a \big). \tag{19}$$

Under these conditions, the system (15) reduces to:

$$\begin{aligned}
&\varphi_1^{(l)} P_l^5 + \varphi_4^{(l)} P_l^3 + \varphi_5^{(l)} \left(\frac{d^2 P_l}{d\xi^2} \right) P_l^2 + \varphi_2^{(l)} P_l^3 P_m^2 \\
&+ \varphi_3^{(l)} P_l P_m^4 + \varphi_{11}^{(l)} P_l P_m^2 + \varphi_6^{(l)} \left(\frac{dP_l}{d\xi} \right)^2 P_l + \varphi_7^{(l)} \left(\frac{dP_m}{d\xi} \right)^2 P_l \\
&+ \varphi_8^{(l)} P_l + \varphi_9^{(l)} \left(\frac{d^2 P_l}{d\xi^2} \right) + \varphi_{10}^{(l)} \left(\frac{d^4 P_l}{d\xi^4} \right) = 0.
\end{aligned} \tag{20}$$

Here, $l = 1, 2$ and $m = 3 - l$. The functions P_l and P_m depend on the similarity variable ξ, whereas $\varphi_i^{(l)}$ $(i = 1, 2, 3, \ldots, 10)$ are arbitrary constants whose explicit expressions are listed in APPENDIX 1.

4. EXACT SOLUTIONS

In this section, we obtain exact solutions of system (1) by solving the reduced system (20) via the Kumar–Malik method. The main steps of the procedure are summarized as follows.

4.1. Kumar-Malik Method

The Kumar–Malik method offers a structured framework for deriving exact analytical solutions of nonlinear differential systems. In brief, the procedure consists of the following steps:

Step 1. Consider a general nonlinear system of ordinary differential equations of the form

$$\mathcal{F}(U, U', U'', U''', \ldots) = 0, \tag{21}$$

where $U = (U_1(\xi),\, U_2(\xi))$ denotes the unknown vector function and the prime ($'$) indicates differentiation with respect to ξ.

Step 2. Assume that each component $U_l(\xi)$ can be represented as a finite polynomial in an auxiliary function $G(\xi)$, namely,

$$U_l(\xi) = B_0^{\{l\}} + B_1^{\{l\}} G(\xi) + B_2^{\{l\}} G^2(\xi) + \cdots + B_{N_l}^{\{l\}} G^{N_l}(\xi), \tag{22}$$

where $B_j^{\{l\}}$ $(j = 0, 1, 2, \ldots, N_l)$ are constants to be determined. The function $G(\xi)$ satisfies the following auxiliary equation:

$$\left(G'(\xi)\right)^2 = \beta_4 G^4(\xi) + \beta_3 G^3(\xi) + \beta_2 G^2(\xi) + \beta_1 G(\xi) + \beta_0, \tag{23}$$

where β_j $(j = 0, 1, 2, 3, 4)$ are arbitrary parameters.

Step 3. The positive integers N_l are determined by applying the homogeneous balance principle, matching the highest-order derivative terms with the dominant nonlinear terms in Eq. (21).

Step 4. Substituting the polynomial ansatz (22) into Eq. (21) and using the auxiliary relation (23) to remove higher-order derivatives of $G(\xi)$ reduces Eq. (21) to a polynomial in $G(\xi)$. By setting the coefficients of identical powers of $G(\xi)$ equal to zero, one obtains an algebraic system for the unknown parameters $B_j^{\{l\}}$. Solving this algebraic system yields explicit expressions for the coefficients.

Finally, inserting the computed constants $B_j^{\{l\}}$ into (22) provides the closed-form expression of $U_l(\xi)$, and hence an exact solution of the original nonlinear system (21).

4.1.1. Family of Solutions to the Auxiliar Equation (23)

In this subsection, we derive explicit solutions of the auxiliary nonlinear ordinary differential equation

$$(G'(\xi))^2 = \beta_4 G^4(\xi) + \beta_3 G^3(\xi) + \beta_2 G^2(\xi) + \beta_1 G(\xi) + \beta_0, \tag{24}$$

in Jacobi elliptic, hyperbolic, and trigonometric forms. The resulting families are classified according to the parameter regimes of β_j $(j = 0, 1, 2, 3, 4)$.
Throughout this work, the quantities Δ_1, Δ_2, Δ_3, and Δ_4 are chosen as:

$$\Delta_1 = 4\beta_2\beta_4 - \beta_3^2, \quad \Delta_2 = 16\beta_2\beta_4 - 5\beta_3^2, \quad \Delta_3 = 8\beta_2\beta_4 - 3\beta_3^2, \quad \Delta_4 = -\frac{\beta_3}{4\beta_4}.$$

Case 1: Assume that $\beta_0 = 0$ and $\beta_1 = \dfrac{\beta_3\Delta_1}{8\beta_4^2}$. Under these assumptions, the auxiliary ODE admits the following Jacobi elliptic function solutions for different parameter conditions:
Sub-case 1.1: If $\beta_4 < 0$ and $\Delta_1 > 0$,

$$G_1(\xi) = \Delta_4 \pm \frac{\beta_3}{4\beta_4}\mathrm{cn}\left(\frac{\sqrt{-\beta_4\Delta_1}\,\xi}{2\beta_4}, \frac{\beta_3}{2\sqrt{\Delta_1}}\right), \tag{25}$$

$$G_2(\xi) = \Delta_4 \pm \frac{\beta_3}{4\beta_4}\mathrm{dn}\left(\frac{\beta_3\xi}{4\sqrt{-\beta_4}}, \frac{2\sqrt{\Delta_1}}{\beta_3}\right). \tag{26}$$

Sub-case 1.2: If $\beta_4 < 0$, $\Delta_1 < 0$, and $\Delta_2 < 0$,

$$G_3(\xi) = \Delta_4 \pm \frac{\sqrt{-\Delta_2}}{4\beta_4}\mathrm{cn}\left(-\frac{\sqrt{\beta_4\Delta_1}\,\xi}{2\beta_4}, \frac{\sqrt{\Delta_1\Delta_2}}{2\Delta_1}\right), \tag{27}$$

$$G_4(\xi) = \Delta_4 \pm \frac{\sqrt{-\Delta_2}}{4\beta_4}\mathrm{dn}\left(-\frac{\sqrt{\beta_4\Delta_2}\,\xi}{4\beta_4}, \frac{2\sqrt{\Delta_1\Delta_2}}{\Delta_2}\right). \tag{28}$$

Sub-case 1.3: If $\beta_4 < 0$, $\Delta_1 > 0$, and $\Delta_2 < 0$,

$$G_5(\xi) = \Delta_4 \pm \frac{\sqrt{-\Delta_2}}{4\beta_4}\mathrm{nc}\left(\frac{\sqrt{-\beta_4\Delta_1}\,\xi}{2\beta_4}, \frac{\beta_3}{2\sqrt{\Delta_1}}\right), \tag{29}$$

$$G_6(\xi) = \Delta_4 \pm \frac{\sqrt{-\Delta_2}}{4\beta_4}\mathrm{nd}\left(-\frac{\beta_3\xi}{4\sqrt{-\beta_4}}, \frac{2\sqrt{\Delta_1}}{\beta_3}\right). \tag{30}$$

Sub-case 1.4: If $\beta_4\Delta_1 > 0$ and $\Delta_1\Delta_2 > 0$,

$$G_7(\xi) = \Delta_4 \pm \frac{\beta_3}{4\beta_4}\mathrm{nc}\left(\frac{\sqrt{\beta_4\Delta_1}\,\xi}{2\beta_4}, \frac{\sqrt{\Delta_1\Delta_2}}{2\Delta_1}\right), \tag{31}$$

$$G_8(\xi) = \Delta_4 \pm \frac{\beta_3}{4\beta_4}\mathrm{nd}\left(\frac{\sqrt{\beta_4\Delta_2}\,\xi}{4\beta_4}, \frac{2\sqrt{\Delta_1\Delta_2}}{\Delta_2}\right). \tag{32}$$

Sub-case 1.5: If $\beta_4 > 0$ and $\Delta_2 < 0$,

$$G_9(\xi) = \Delta_4 \pm \frac{\beta_3}{4\beta_4}\mathrm{ns}\left(-\frac{\beta_3\xi}{4\sqrt{\beta_4}}, \frac{\sqrt{-\Delta_2}}{\beta_3}\right), \tag{33}$$

$$G_{10}(\xi) = \Delta_4 \pm \frac{\sqrt{-\Delta_2}}{4\beta_4}\mathrm{ns}\left(-\frac{\sqrt{-\beta_4\Delta_2}\,\xi}{4\beta_4}, \frac{\beta_3}{\sqrt{-\Delta_2}}\right), \tag{34}$$

$$G_{11}(\xi) = \Delta_4 \pm \frac{\beta_3}{4\beta_4}\mathrm{sn}\left(-\frac{\beta_3\xi}{4\sqrt{\beta_4}}, \frac{\sqrt{-\Delta_2}}{\beta_3}\right), \tag{35}$$

$$G_{12}(\xi) = \Delta_4 \pm \frac{\sqrt{-\Delta_2}}{4\beta_4}\mathrm{sn}\left(-\frac{\sqrt{-\beta_4\Delta_2}\,\xi}{4\beta_4}, \frac{\beta_3}{\sqrt{-\Delta_2}}\right). \tag{36}$$

Case 2: $\beta_0 = \frac{\Delta_1^2}{64\beta_4^3}$, $\beta_1 = \frac{\beta_3\Delta_1}{8\beta_4^2}$. Then the auxiliary ODE admits the following hyperbolic, and trigonometric function solutions under different conditions:

Sub-case 2.1: $\beta_4 > 0$, $\Delta_3 < 0$

$$G_{13}(\xi) = \Delta_4 \pm \frac{\sqrt{-\Delta_3}}{4\beta_4}\tanh\left(\frac{\sqrt{-\beta_4\Delta_3}\,\xi}{4\beta_4}\right), \tag{37}$$

$$G_{14}(\xi) = \Delta_4 \pm \frac{\sqrt{-\Delta_3}}{4\beta_4}\coth\left(\frac{\sqrt{-\beta_4\Delta_3}\,\xi}{4\beta_4}\right). \tag{38}$$

Sub-case 2.2: $\beta_4 > 0$, $\Delta_3 > 0$

In this case, the resulting solutions are periodic and fall outside the scope of the present study; hence, they are omitted.

Case 3: $\beta_0 = \frac{\beta_3^2\Delta_2}{256\beta_4^3}$, $\beta_1 = \frac{\beta_3\Delta_1}{8\beta_4^2}$. Under these conditions, the auxiliary ODE admits the following hyperbolic and trigonometric function solutions for various parameter regimes:

Sub-case 3.1: $\beta_4 < 0$, $\Delta_3 < 0$

$$G_{17}(\xi) = \Delta_4 \pm \frac{\sqrt{-2\Delta_3}}{4\beta_4}\mathrm{sech}\left(\frac{\sqrt{2\beta_4\Delta_3}\,\xi}{4\beta_4}\right). \tag{39}$$

Sub-case 3.2: $\beta_4 > 0, \Delta_3 > 0$

$$G_{18}(\xi) = \Delta_4 \pm \frac{\sqrt{2\Delta_3}}{4\beta_4}\operatorname{csch}\left(\frac{\sqrt{2\beta_4\Delta_3}\,\xi}{4\beta_4}\right). \tag{40}$$

Sub-case 3.3: $\beta_4 > 0, \Delta_3 < 0$

In this case, the corresponding solutions are beyond the scope of the present work and are therefore not presented.

Case 4: $\beta_0 = 0, \beta_1 = 0, \beta_3 = 0$

$$G_{21}(\xi) = \frac{4\rho\beta_2}{4\rho^2 e^{\sqrt{\beta_2}\xi} - \beta_4\beta_2 e^{-\sqrt{\beta_2}\xi}}. \tag{41}$$

4.2. Application of Kumar-Malik Method

Assume that the solution of Eq. (20) is sought in the form:

$$P_l(\xi) = A_0^{(l)} + A_1^{(l)}R(\xi) + A_2^{(l)}R^2(\xi) + A_3^{(l)}R^3(\xi) + \dots + A_{N_l}^{(l)}R^{N_l}(\xi), \tag{42}$$

where $l = 1, 2$. Substituting the ansatz (42) with $N_l = 1$ into the reduced system (20), and following the procedure outlined in Section 4.1, we obtain two polynomial expressions in $R(\xi)$. Equating to zero the coefficients of each power of $R(\xi)$ (together with the constant terms) produces an algebraic system for the unknown parameters. Solving this system yields the following values:

$$A_0^{(1)} = -\frac{\beta_3\sqrt{30}\,\vartheta_1}{4\beta_4\,\vartheta_2}, \quad A_1^{(1)} = \frac{4A_0^{(1)}}{\beta_3},$$

$$A_0^{(2)} = -\frac{\beta_3\sqrt{30}\sqrt{\beta_4\vartheta_3\,\sigma_7\sigma_{12}\left((\alpha_1+\gamma_1)\sigma_{12}+\lambda_2\sigma_{11}\right)}\,\varrho_1}{4\beta_4\,\vartheta_3}, \quad A_1^{(2)} = \frac{4A_0^{(2)}}{\beta_3}\,\vartheta_3,$$

$$b_1 = \frac{-160F_1\beta c_{12}\sigma_{12}^3\varrho_1^2 + 80F_4 a\beta_4\sigma_{11}^2\sigma_7 + F_2\sigma_{12}^2 + F_3\sigma_{11}\sigma_{12}}{240\,\beta_4\,\sigma_7\,\sigma_{12}\,\sigma_{11}\left(\sigma_{11}(\alpha_2+\gamma_2) - \lambda_1\sigma_{12}\right)},$$

$$b_2 = \frac{-160F_{11}\beta c_{12}\sigma_{12}^3\varrho_1^2 - 80F_{44}a\beta_4\sigma_{11}\sigma_7 + F_{22}\sigma_{12}^2 + F_{33}\sigma_{12}}{240\,\beta_4\,\sigma_7\,\sigma_{12}\left(\sigma_{12}(\alpha_1+\gamma_1) - \lambda_2\sigma_{11}\right)},$$

$$\delta_1 = \frac{\sigma_{11}^2\left(E_1\,\sigma_{12} + 2E_2\,\sigma_7\right) - \sigma_{11}\sigma_{12}\left(E_3\,\sigma_{12} + E_4\,\sigma_7\right) + \sigma_{12}^2\sigma_7 E_5}{\sigma_7\,\sigma_{12}\left[-\lambda_1\sigma_{12} + \sigma_{11}(\alpha_2+\gamma_2)\right]},$$

$$f_1 = \frac{X_7\,\sigma_{12}^4 + X_8\,\sigma_{12}^3 + X_9\,\sigma_{12}^2 + \left(16\,X_1\,\sigma_{11}^3\,\sigma_7\,(\alpha_2+\gamma_2)(\tau_2+\theta_2) + 6\,X_1X_2\,\sigma_{11}^2\,\sigma_7^2\right)\sigma_{12} + 8\,X_1^2\,\sigma_{11}^3\,\sigma_7^2}{50\,\sigma_7^2\,\sigma_{12}^2\left(\sigma_{11}(\alpha_2+\gamma_2) - \lambda_1\sigma_{12}\right)^2},$$

$$f_2 = \frac{8\,\lambda_1^2\,\sigma_{12}^4\,(\tau_2+\theta_2)^2 + 50\,X_{10}\,\lambda_1\,\sigma_{12}^3 + X_{11}\,\sigma_{12}^2 + 50\,X_{12}\,\sigma_{11}\,\sigma_7\,\sigma_{12} + 8\,X_1^2\,\sigma_{11}^2\,\sigma_7^2}{50\,\sigma_7^2\,\sigma_{12}\left(\lambda_2\sigma_{11} - (\alpha_1+\gamma_1)\sigma_{12}\right)^2},$$

$$\kappa = \sqrt{\frac{2\left[\left(\frac{3\beta_3^2}{8} - \beta_2\beta_4\right)c_{12}\varrho_1^2\sigma_{12} - a\beta_4\right]}{c_{12}\sigma_{12}\beta_4}}$$

$$\omega = \frac{18432\,\lambda_1\varrho_1^4c_{12}^2\sigma_{12}^4(\tau_2+\theta_2)Z_1 + 4608\,\varrho_1^4c_{12}^2\sigma_{12}^3Z_5 - \sigma_{12}^2Z_6 - 128\,a^2\beta_2^2\sigma_{12}Z_7 - 128\,\sigma_7a^2\sigma_{11}\beta_4^2Z_2}{1536\,\sigma_{12}\beta_4^2c_{12}\left(\lambda_1\sigma_{12}^2(\tau_2+\theta_2) - \sigma_{12}Z_7 - \sigma_7\sigma_{11}Z_2\right)}.$$

See **??** for further details. Substituting the above parameter values into the similarity form (14), the solution of Eq. (1) can be written as:

$$\begin{aligned} q(t,x) &= P_1(t,x)e^{i(-\kappa x+\omega t+\theta_0)}, \\ r(t,x) &= P_2(t,x)e^{i(-\kappa x+\omega t+\theta_0)}, \end{aligned} \tag{43}$$

where the functions $P_l(t,x)$ $(l = 1,2)$ are specified in the cases listed below.
Throughout this paper, the constants $C_{0,l}$ and $C_{1,l}$ are defined by:

$$C_{0,l} = \begin{cases} A_0^{(1)}, & l = 1, \\ A_0^{(2)}, & l = 2, \end{cases} \quad C_{1,l} = \begin{cases} A_1^{(1)}, & l = 1, \\ A_1^{(2)}, & l = 2. \end{cases}$$

Case 1: Assume that $\beta_0 = 0$ and

$$\beta_1 = \frac{\beta_3\left(4\beta_2\beta_4 - \beta_3^2\right)}{8\beta_4^2}.$$

Under these assumptions, $P_l(t,x)$ admits the following Jacobi elliptic function solutions:
Sub-case 1.1: If $\beta_4 < 0$ and $\Delta_1 > 0$, then

$$P_l^{(1)}(t,x) = C_{0,l} + C_{1,l}\left(\Delta_4 \pm \frac{\beta_3}{4\beta_4}\,\mathrm{cn}\left(\frac{\sqrt{-\beta_4\Delta_1}\,(\varrho_1 x - \varrho_2 t)}{2\beta_4}, \frac{\beta_3}{2\sqrt{\Delta_1}}\right)\right), \tag{44}$$

$$P_l^{(2)}(t,x) = C_{0,l} + C_{1,l}\left(\Delta_4 \pm \frac{\beta_3}{4\beta_4}\,\mathrm{dn}\left(\frac{\beta_3(\varrho_1 x - \varrho_2 t)}{4\sqrt{-\beta_4}}, \frac{2\sqrt{\Delta_1}}{\beta_3}\right)\right). \tag{45}$$

Sub-case 1.2: If $\beta_4 < 0$, $\Delta_1 < 0$, and $\Delta_2 < 0$,

$$P_l^{(3)}(t,x) = C_{0,l} + C_{1,l}\left(\Delta_4 \pm \frac{\sqrt{-\Delta_2}}{4\beta_4}\mathrm{cn}\left(-\frac{\sqrt{\beta_4\Delta_1}\,(\varrho_1 x - \varrho_2 t)}{2\beta_4}, \frac{\sqrt{\Delta_1\Delta_2}}{2\Delta_1}\right)\right), \tag{46}$$

$$P_l^{(4)}(t,x) = C_{0,l} + C_{1,l}\left(\Delta_4 \pm \frac{\sqrt{-\Delta_2}}{4\beta_4}\mathrm{dn}\left(-\frac{\sqrt{\beta_4\Delta_2}\,(\varrho_1 x - \varrho_2 t)}{4\beta_4}, \frac{2\sqrt{\Delta_1\Delta_2}}{\Delta_2}\right)\right). \tag{47}$$

Sub-case 1.3: If $\beta_4 < 0$, $\Delta_1 > 0$, and $\Delta_2 < 0$,

$$P_l^{(5)}(t,x) = C_{0,l} + C_{1,l}\left(\Delta_4 \pm \frac{\sqrt{-\Delta_2}}{4\beta_4}\mathrm{nc}\left(\frac{\sqrt{-\beta_4\Delta_1}\,(\varrho_1 x - \varrho_2 t)}{2\beta_4}, \frac{\beta_3}{2\sqrt{\Delta_1}}\right)\right), \tag{48}$$

$$P_l^{(6)}(t,x) = C_{0,l} + C_{1,l}\left(\Delta_4 \pm \frac{\sqrt{-\Delta_2}}{4\beta_4}\mathrm{nd}\left(-\frac{\beta_3(\varrho_1 x - \varrho_2 t)}{4\sqrt{-\beta_4}}, \frac{2\sqrt{\Delta_1}}{\beta_3}\right)\right). \tag{49}$$

Sub-case 1.4: If $\beta_4\Delta_1 > 0$ and $\Delta_1\Delta_2 > 0$,

$$P_l^{(7)}(t,x) = C_{0,l} + C_{1,l}\left(\Delta_4 \pm \frac{\beta_3}{4\beta_4}\mathrm{nc}\left(\frac{\sqrt{\beta_4\Delta_1}\,(\varrho_1 x - \varrho_2 t)}{2\beta_4}, \frac{\sqrt{\Delta_1\Delta_2}}{2\Delta_1}\right)\right), \tag{50}$$

$$P_l^{(8)}(t,x) = C_{0,l} + C_{1,l}\left(\Delta_4 \pm \frac{\beta_3}{4\beta_4}\mathrm{nd}\left(\frac{\sqrt{\beta_4\Delta_2}\,(\varrho_1 x - \varrho_2 t)}{4\beta_4}, \frac{2\sqrt{\Delta_1\Delta_2}}{\Delta_2}\right)\right). \tag{51}$$

Sub-case 1.5: If $\beta_4 > 0$ and $\Delta_2 < 0$,

$$P_l^{(9)}(t,x) = C_{0,l} + C_{1,l}\left(\Delta_4 \pm \frac{\beta_3}{4\beta_4}\mathrm{ns}\left(-\frac{\beta_3(\varrho_1 x - \varrho_2 t)}{4\sqrt{\beta_4}}, \frac{\sqrt{-\Delta_2}}{\beta_3}\right)\right), \tag{52}$$

$$P_l^{(10)}(t,x) = C_{0,l} + C_{1,l}\left(\Delta_4 \pm \frac{\sqrt{-\Delta_2}}{4\beta_4}\mathrm{ns}\left(-\frac{\sqrt{-\beta_4\Delta_2}\,(\varrho_1 x - \varrho_2 t)}{4\beta_4}, \frac{\beta_3}{\sqrt{-\Delta_2}}\right)\right), \tag{53}$$

$$P_l^{(11)}(t,x) = C_{0,l} + C_{1,l}\left(\Delta_4 \pm \frac{\beta_3}{4\beta_4}\mathrm{sn}\left(-\frac{\beta_3(\varrho_1 x - \varrho_2 t)}{4\sqrt{\beta_4}}, \frac{\sqrt{-\Delta_2}}{\beta_3}\right)\right), \tag{54}$$

$$P_l^{(12)}(t,x) = C_{0,l} + C_{1,l}\left(\Delta_4 \pm \frac{\sqrt{-\Delta_2}}{4\beta_4}\mathrm{sn}\left(-\frac{\sqrt{-\beta_4\Delta_2}\,(\varrho_1 x - \varrho_2 t)}{4\beta_4}, \frac{\beta_3}{\sqrt{-\Delta_2}}\right)\right). \tag{55}$$

Case 2: $\beta_0 = \frac{\Delta_1^2}{64\beta_4^3}$, $\beta_1 = \frac{\beta_3\Delta_1}{8\beta_4^2}$. Under these conditions, $P_l(t,x)$ admits the following hyperbolic and trigonometric function solutions for the corresponding parameter regimes: *Sub-case 2.1:* $\beta_4 > 0$, $\Delta_3 < 0$

$$P_l^{(13)}(t,x) = C_{0,l} + C_{1,l}\left(\Delta_4 \pm \frac{\sqrt{-\Delta_3}}{4\beta_4}\tanh\left(\frac{\sqrt{-\beta_4\Delta_3}\,(\varrho_1 x - \varrho_2 t)}{4\beta_4}\right)\right), \tag{56}$$

$$P_l^{(14)}(t,x) = C_{0,l} + C_{1,l}\left(\Delta_4 \pm \frac{\sqrt{-\Delta_3}}{4\beta_4}\coth\left(\frac{\sqrt{-\beta_4\Delta_3}\,(\varrho_1 x - \varrho_2 t)}{4\beta_4}\right)\right). \quad (57)$$

Sub-case 2.2: $\beta_4 > 0, \Delta_3 > 0$

In this case, the solutions are periodic; since they are not central to the objectives of this study, they are not pursued further.

Case 3: $\beta_0 = \frac{\beta_3^2\Delta_2}{256\beta_4^3}, \beta_1 = \frac{\beta_3\Delta_1}{8\beta_4^2}$. Accordingly, $P_l(t,x)$ admits the following hyperbolic and trigonometric solutions under the associated parameter conditions:

Sub-case 3.1: $\beta_4 < 0, \Delta_3 < 0$

$$P_l^{(17)}(t,x) = C_{0,l} + C_{1,l}\left(\Delta_4 \pm \frac{\sqrt{-2\Delta_3}}{4\beta_4}\operatorname{sech}\left(\frac{\sqrt{2\beta_4\Delta_3}\,(\varrho_1 x - \varrho_2 t)}{4\beta_4}\right)\right). \quad (58)$$

Sub-case 3.2: $\beta_4 > 0, \Delta_3 > 0$

$$P_l^{(18)}(t,x) = C_{0,l} + C_{1,l}\left(\Delta_4 \pm \frac{\sqrt{2\Delta_3}}{4\beta_4}\operatorname{csch}\left(\frac{\sqrt{2\beta_4\Delta_3}\,(\varrho_1 x - \varrho_2 t)}{4\beta_4}\right)\right). \quad (59)$$

Sub-case 3.3: $\beta_4 > 0, \Delta_3 < 0$

Although this case yields periodic waveforms, they are not relevant to the aims of the present analysis and are therefore omitted.

Case 4: $\beta_0 = 0, \beta_1 = 0, \beta_3 = 0, \beta_2 > 0$

$$P_l^{(21)}(t,x) = C_{0,l} + C_{1,l}\left(\frac{4\rho\beta_2}{4\rho^2 e^{\sqrt{\beta_2}(\varrho_1 x - \varrho_2 t)} - \beta_4\beta_2 e^{-\sqrt{\beta_2}(\varrho_1 x - \varrho_2 t)}}\right). \quad (60)$$

5. GRAPHICAL REPRESENTATION AND PHYSICAL INTERPRETATION

In this section, we examine the spatiotemporal evolution of the coupled complex fields $q(x,t)$ and $r(x,t)$ arising from the general traveling–wave representation (43), using two distinct closed-form choices for the amplitude functions. Specifically, we consider the dark-soliton profiles given in (56) and the bright-soliton profiles given in (58). For visualization, we display the corresponding intensities $|q(x,t)|^2$ and $|r(x,t)|^2$ using 3D surface plots, contour maps, and 2D cross-sections at several fixed time levels.

5.1. Dark Soliton Dynamics

Figure 1 displays the intensity distributions obtained by inserting (56) into the traveling–wave form (43). The resulting dark-soliton profile is characterized by an intensity dip superimposed on a nonzero continuous background. This localized notch travels along the trajectory specified by the wave variable $\xi = \varrho_1 x - \varrho_2 t$, which appears in the contour plots as an oblique band marking the transition region. Such behavior is typical of dark solitons: the field approaches a finite pedestal as $|\xi| \to \infty$, while the dispersion–nonlinearity balance sustains a stable localized depression that retains its shape during propagation. From a physical viewpoint, dark solitons are commonly associated with defocusing nonlinear regimes (or an effective defocusing response in coupled settings), where the nonlinear interaction supports a robust dip on a finite background rather than a localized peak.

5.2. Bright Soliton Dynamics

Figure 2 depicts the spatiotemporal behavior obtained by substituting (58) into the traveling–wave expression (43). Unlike the dark-soliton case, the bright-soliton profile exhibits a *localized intensity peak* that attains its maximum near the soliton core and decays rapidly as $|\xi|$ increases. In the contour maps, this structure appears as a thin ridge propagating along the characteristic direction prescribed by $\xi = \varrho_1 x - \varrho_2 t$, indicating a coherent pulse traveling with the corresponding wave speed. This is the defining signature of a bright soliton, namely a self-confined wave packet sustained by the balance between dispersion (or diffraction) and nonlinear self-focusing. Physically, bright solitons are typically supported in focusing nonlinear regimes (or in coupled systems with an effective focusing response), where the nonlinear interaction counteracts dispersive spreading and maintains a stable localized hump.

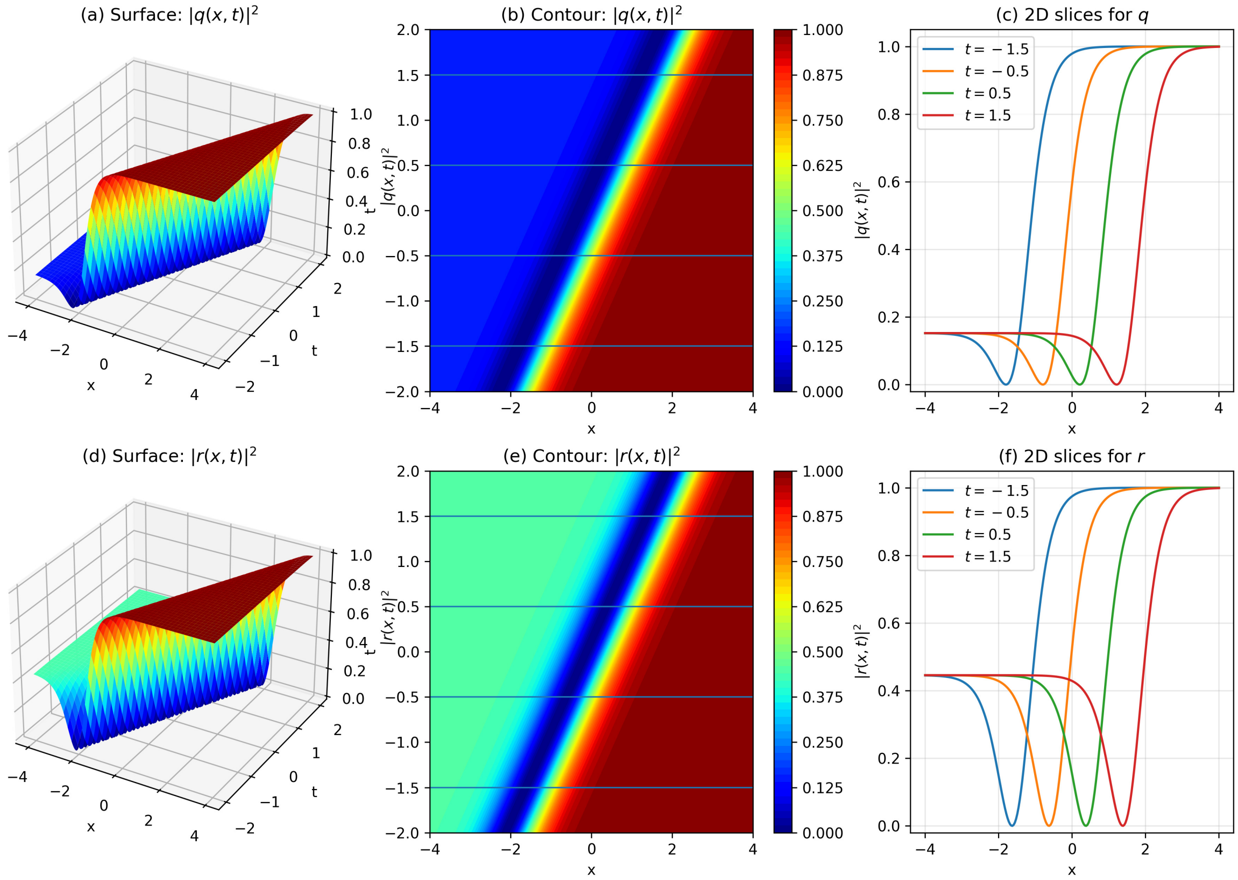

Figure 1. Surface (left), contour (middle), and 2D profiles (right) of the coupled fields $q(x,t)$ and $r(x,t)$ corresponding to the analytical solution (43) constructed from the dark soliton solution (56). The first row depicts $|q(x,t)|^2$, while the second row depicts $|r(x,t)|^2$. The 2D panels show $|q(x,t)|^2$ and $|r(x,t)|^2$ as functions of x at several fixed time instants (as indicated in the legends), and the same time levels are marked on the contour plots for reference.

5.3. Comparison and Physical Meaning

A comparison of Figures 1 and 2 reveals the qualitative distinctions between the two solution classes:

- **Background behavior:** The dark-soliton pattern propagates as an intensity *depression* on a finite continuous background, whereas the bright-soliton pattern manifests as a localized intensity *hump* that decays rapidly away from its center.

- **Type of localization:** The bright soliton is localized through spatial confinement of a peak, while the dark soliton is localized via a notch embedded in a nonzero pedestal.

- **Propagation characteristics:** In both cases, the waveforms translate along the traveling variable $\xi = \varrho_1 x - \varrho_2 t$ without distortion, with an effective speed determined by ϱ_2/ϱ_1.

- **Coupled-field features:** The two intensities $|q|^2$ and $|r|^2$ exhibit the same traveling structure, but their amplitudes and offsets can differ according to the free parameters in (43), indicating how the coupling redistributes energy between the polarization modes.

Hence, the two functional profiles describe distinct nonlinear propagation regimes within the same coupled framework: a dark-soliton regime characterized by intensity depletion on a continuous-wave background, and a bright-soliton regime characterized by a self-confined pulse supported by effective focusing. The numerical visualizations corroborate the solitonic character of the derived closed-form solutions and demonstrate that the selected amplitude profile governs the qualitative propagation physics in the modeled birefringent medium.

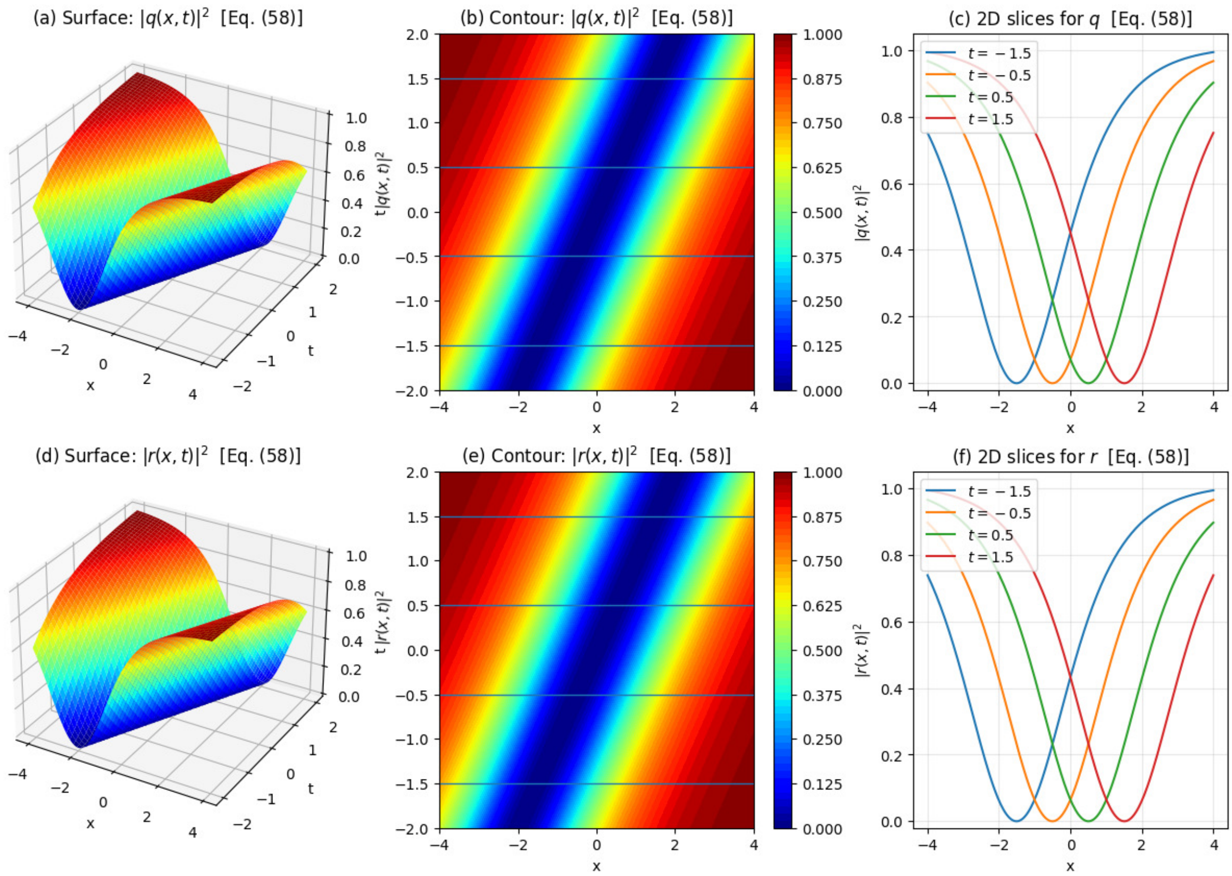

Figure 2. Surface (left), contour (middle), and 2D profiles (right) of the coupled fields $q(x,t)$ and $r(x,t)$ corresponding to the analytical solution (43) constructed from the bright soliton solution (58). The first row depicts $|q(x,t)|^2$, while the second row depicts $|r(x,t)|^2$. The 2D panels show $|q(x,t)|^2$ and $|r(x,t)|^2$ as functions of x at several fixed time instants (as indicated in the legends), and the same time levels are marked on the contour plots for reference.

6. CONCLUSIONS

In this work, we investigated a generalized concatenation model for birefringent optical fibers and derived new exact soliton solutions. By means of Lie symmetry analysis, the coupled nonlinear evolution equations were reduced, through appropriate similarity variables, to a tractable system of ordinary differential equations. The reduced system was then solved analytically using the Kumar–Malik method, which produced several families of closed-form solutions expressed in Jacobi elliptic, hyperbolic, and trigonometric functions. For suitable parameter constraints, these solution families degenerate to the standard bright-, dark-, and periodic-soliton regimes, thereby demonstrating that the model supports qualitatively distinct waveform classes within a unified higher-order coupled framework. Representative graphical illustrations further confirmed the physical relevance of the obtained structures and highlighted the influence of parameters on the propagation characteristics.

Overall, the combination of symmetry reduction and the Kumar–Malik technique provides an efficient analytical route for exploring higher-order coupled optical systems. The explicit solutions reported here can serve as benchmark test cases for numerical simulations and may facilitate further theoretical studies. Possible extensions include the investigation of perturbed or fractional forms of the concatenation model, the derivation of conservation laws, and a detailed analysis of modulation instability, as well as interaction dynamics among solitons, breathers, and other localized waveforms in birefringent media.

Funding: This research received no external funding.

Acknowledgments: The author, Rajveer Singh, is very much thankful to UGC for providing financial support in the form of SRF fellowship via letter UGC ID: 211610023103. The author, Sachin Kumar, wants to acknowledge the financial

support provided under the scheme "Fund for Improvement of S&T Infrastructure (FIST)" of the Department of Science & Technology (DST), Government of India via letter no. SR/FST/MS-I/2021/104 to the Department of Mathematics and Statistics, Central University of Punjab.
This work was funded from the budget of Grambling State University for the Endowed Chair of Mathematics. No additional grants have been received to conduct or direct this particular study.

Conflicts of interest: The authors declare no conflicts of interest.

APPENDIX 1

$$\varphi_1^{(l)} = \begin{cases} c_{12}\,\sigma_{12}\,\sigma_7\,f_1, & l=1\\ c_{12}\,\sigma_7\,f_2, & l=2 \end{cases}$$

$$\varphi_2^{(l)} = \begin{cases} c_{12}\,\sigma_{12}\,\sigma_7\,g_1, & l=1\\ c_{12}\,\sigma_7\,g_2, & l=2 \end{cases}$$

$$\varphi_3^{(l)} = \begin{cases} c_{12}\,\sigma_{12}\,\sigma_7\,h_1, & l=1\\ c_{12}\,\sigma_7\,h_2, & l=2 \end{cases}$$

$$\varphi_4^{(l)} = \begin{cases} c_{12}\,\kappa^2\,\sigma_{12}(\alpha_1+\delta_1+\gamma_1-3\mu_1)+b_1\sigma_{11}\sigma_7-8c_{12}\kappa^2\sigma_{11}\sigma_{12}\varepsilon_1, & l=1\\ c_{12}\,\kappa^2(\alpha_2+\delta_2+\gamma_2-3\mu_2)+b_2\sigma_7-8c_{12}\kappa^2\sigma_{12}\varepsilon_2, & l=2 \end{cases}$$

$$\varphi_5^{(l)} = \begin{cases} c_{12}\,\sigma_{12}\,\sigma_7\,\varrho_1^2(\delta_1+\mu_1), & l=1\\ c_{12}\,\sigma_7\,\varrho_1^2(\delta_2+\mu_2), & l=2 \end{cases}$$

$$\varphi_6^{(l)} = \begin{cases} c_{12}\,\sigma_{12}\,\sigma_7(\alpha_1+\gamma_1)\varrho_1^2, & l=1\\ c_{12}\,\sigma_7(\alpha_2+\gamma_2)\varrho_1^2, & l=2 \end{cases}$$

$$\varphi_7^{(l)} = \begin{cases} \lambda_1\,\sigma_{12}\,\varrho_1^2\,c_{12}\,\sigma_7, & l=1\\ \lambda_2\,\varrho_1^2\,c_{12}\,\sigma_7, & l=2 \end{cases}$$

$$\varphi_8^{(l)} = \begin{cases} -3c_{12}\kappa^4\sigma_{11}\sigma_{12}\sigma_7-a\kappa^2\sigma_{11}\sigma_7-\omega\sigma_{11}\sigma_7, & l=1\\ -3c_{12}\kappa^4\sigma_{12}\sigma_7-a\kappa^2\sigma_7-\omega\sigma_7, & l=2 \end{cases}$$

$$\varphi_9^{(l)} = \begin{cases} 6c_{12}\kappa^2\sigma_{11}\sigma_{12}\varrho_1^2+a\sigma_{11}\sigma_7\varrho_1^2, & l=1\\ 6c_{12}\kappa^2\sigma_{12}\sigma_7\varrho_1^2+a\sigma_7\varrho_1^2, & l=2 \end{cases}$$

$$\varphi_{10}^{(l)} = \begin{cases} \sigma_{11}\sigma_{12}\varrho_1^4c_{12}\sigma_7, & l=1\\ \sigma_{12}\varrho_1^4c_{12}\sigma_7, & l=2 \end{cases}$$

$$\varphi_{11}^{(l)} = \begin{cases} c_{12}\kappa^2\sigma_{12}\sigma_7\lambda_1-2c_{12}\kappa^2\sigma_{12}\sigma_7\rho_1-6c_{12}\kappa^2\sigma_{11}\sigma_{12}\tau_1+2c_{12}\kappa^2\sigma_{11}\sigma_{12}\theta_1+c_1\sigma_{11}\sigma_7, & l=1\\ c_{12}\kappa^2\sigma_7\lambda_2-2c_{12}\kappa^2\sigma_7\rho_2-6c_{12}\kappa^2\sigma_{12}\tau_2+2c_{12}\kappa^2\sigma_{12}\theta_2+c_2\sigma_7. & l=2 \end{cases}$$

APPENDIX 2
APPLICATION OF KUMAR-MALIK METHOD

Let the solution of Eq. (20) takes the form:

$$P_l(\xi) = A_0^{(l)} + A_1^{(l)}R(\xi) + A_2^{(l)}R^2(\xi) + A_3^{(l)}R^3(\xi) + \dots + A_{N_l}^{(l)}R^{N_l}(\xi), \tag{61}$$

where $l = 1, 2$. Substituting Eq. (61) with $N_l = 1$ into system (20), and using procedure mentioned in Section 4.1, we arrive at two polynomial equations in $R(\xi)$. Setting the coefficients of powers of $R(\xi)$, combined with the constant terms, to zero yields the system of equations, after solving that system gives the values of $A_0^{(1)}, A_1^{(1)}, A_0^{(2)}, A_1^{(2)}, b_1, b_2, \delta_1, f_1, f_2$ and ω as follows:

- $A_0^{(1)} = -\dfrac{\beta_3\sqrt{30}\,\vartheta_1}{4\beta_4\,\vartheta_2}, \quad A_1^{(1)} = \dfrac{4A_0^{(1)}}{\beta_3},$

  $A_0^{(2)} = -\dfrac{\beta_3\sqrt{30}\,\sqrt{\beta_4\vartheta_3\,\sigma_7\sigma_{12}\left((\alpha_1+\gamma_1)\sigma_{12}+\lambda_2\sigma_{11}\right)}\,\varrho_1}{4\beta_4\,\vartheta_3}, \quad A_1^{(2)} = \dfrac{4A_0^{(2)}\,\vartheta_3}{\beta_3}$

  where

$$\begin{aligned}
\vartheta_1 &= \sqrt{\beta_4\,\varrho_1^2\,\sigma_7\sigma_{12}\left(\sigma_{11}(\alpha_2+\gamma_2)-\lambda_1\sigma_{12}\right)},\\
\vartheta_2 &= \left((\tau_2+\theta_2)\sigma_{11}+(\alpha_1+\gamma_1)\sigma_7\right)\sigma_{12}+\rho_2\sigma_{11}\sigma_7,\\
\vartheta_3 &= 2\lambda_1(\tau_2+\theta_2)\sigma_{12}^2+\Big[\big((-2\alpha_1-2\gamma_1)\alpha_2+(-2\alpha_1-2\gamma_1)\gamma_2+(2\lambda_2+2\rho_2)\lambda_1-(\alpha_1+\gamma_1)(\mu_2+\delta_2)\big)\sigma_7\\
&\quad-2\sigma_{11}(\alpha_2+\gamma_2)(\tau_2+\theta_2)\Big]\sigma_{12}+\sigma_{11}(-2\rho_2\alpha_2-2\rho_2\gamma_2+\lambda_2(\mu_2+\delta_2))\sigma_7.
\end{aligned} \tag{62}$$

- $b_1 = \dfrac{-160F_1\beta c_{12}\sigma_{12}^3\varrho_1^2+80F_4 a\beta_4\sigma_{11}^2\sigma_7+F_2\sigma_{12}^2+F_3\sigma_{11}\sigma_{12}}{240\,\beta_4\,\sigma_7\,\sigma_{12}\,\sigma_{11}\left(\sigma_{11}(\alpha_2+\gamma_2)-\lambda_1\sigma_{12}\right)},$

  $b_2 = \dfrac{-160F_{11}\beta c_{12}\sigma_{12}^3\varrho_1^2-80F_{44}a\beta_4\sigma_{11}\sigma_7+F_{22}\sigma_{12}^2+F_{33}\sigma_{12}}{240\,\beta_4\,\sigma_7\,\sigma_{12}\left(\sigma_{12}(\alpha_1+\gamma_1)-\lambda_2\sigma_{11}\right)}$

where

$$\begin{aligned}
F_1 &= \Big[\big(-\tfrac{7\theta_2}{10}-2\varepsilon_1-\tfrac{7\tau_2}{10}\big)\lambda_1+2\tau_1(\alpha_1+\gamma_1)\Big]\sigma_{11}+\sigma_7\big[-\mu_1\lambda_1+\rho_1(\alpha_1+\gamma_1)\big],\\
F_{11} &= 2\varepsilon_2(\alpha_1+\gamma_1)-\tfrac{7}{10}(\theta_2+\tfrac{27\tau_2}{7})\lambda_1,\\
F_2 &= -112\,c_{12}\,\beta\,\varrho_1^2\,\sigma_{11}^2\Big[(\tau_2+\theta_2+\tfrac{20\varepsilon_1}{7})(\alpha_2+\gamma_2)-\tfrac{20\tau_1\lambda_2}{7}\Big]\\
&\quad+88\,c_{12}\,\beta_2\,\sigma_7\,\varrho_1^2\Big[(\alpha_1+\gamma_1-\tfrac{20\mu_1}{11})(\alpha_2+\gamma_2)+(-\lambda_2+\tfrac{14\rho_2}{11})\lambda_1+(-\tfrac{7\delta_2}{11}-\tfrac{7\mu_2}{11})(\alpha_1+\gamma_1)+\tfrac{20\rho_1\lambda_2}{11}\Big]\\
&\quad-240\,c_1\,\sigma_7\,(\alpha_1+\gamma_1)-320\,a\,\beta_4\Big[\big(\tfrac{\theta_2}{4}-\varepsilon_1+\tfrac{\tau_2}{4}\big)\lambda_1+\tau_1(\alpha_1+\gamma_1)\Big]\\
&\quad-33\,c_{12}\,\beta_3^2\,\sigma_7\,\varrho_1^2\Big[(\alpha_1+\gamma_1-\tfrac{20\mu_1}{11})(\alpha_2+\gamma_2)+(-\lambda_2+\tfrac{14\rho_2}{11})\lambda_1+(-\tfrac{7\delta_2}{11}-\tfrac{7\mu_2}{11})(\alpha_1+\gamma_1)+\tfrac{20\rho_1\lambda_2}{11}\Big]\sigma_{11}\\
&\quad-160\,a\,\beta_4\,\sigma_7\big[-\mu_1\lambda_1+\rho_1(\alpha_1+\gamma_1)\big],\\
F_{22} &= 88\,c_{12}\,\beta_2\,\varrho_1^2\,\sigma_7\Big[(\gamma_2-\tfrac{27\mu_2}{11}+\alpha_2-\tfrac{7\delta_2}{11})\alpha_1+\alpha_2\gamma_1+(\gamma_2-\tfrac{27\mu_2}{11}-\tfrac{7\delta_2}{11})\gamma_1-\lambda_1(\lambda_2-\tfrac{34\rho_2}{11})\Big]\\
&\quad-\tfrac{14}{11}\,c_{12}\,\beta_2\,\sigma_{11}\,\varrho_1^2\Big[(\theta_2+\tfrac{27\tau_2}{7})(\alpha_2+\gamma_2)-\tfrac{20\lambda_2\varepsilon_2}{7}\Big]\\
&\quad+240\,c_2\,\sigma_7\,\lambda_1\,\beta_4-320\,a\,\beta_4\Big[\varepsilon_2(\alpha_1+\gamma_1)+\lambda_1\tfrac{(\theta_2-3\tau_2)}{4}\Big]\\
&\quad-33\,c_{12}\,\beta_3^2\,\varrho_1^2\Big[(\gamma_2-\tfrac{27\mu_2}{11}+\alpha_2-\tfrac{7\delta_2}{11})\alpha_1+\alpha_2\gamma_1+(\gamma_2-\tfrac{27\mu_2}{11}-\tfrac{7\delta_2}{11})\gamma_1\\
&\quad-\lambda_1(\lambda_2-\tfrac{34\rho_2}{11})-\tfrac{14\sigma_{11}}{11}\Big[(\theta_2+\tfrac{27\tau_2}{7})(\alpha_2+\gamma_2)-\tfrac{20\lambda_2\varepsilon_2}{7}\Big]\Big],\\
F_3 &= -\tfrac{14}{5}\,c_{12}\,\beta_2\,\beta_4\,\sigma_7\,\varrho_1^2\big[\rho_2(\alpha_2+\gamma_2)-\tfrac{\lambda_2(\mu_2+\delta_2)}{2}\big]+6\,c_1\,\sigma_7\,\lambda_2\,\beta_4\\
&\quad+2\,a\,\beta_4\Big[(\tau_2+\theta_2-4\varepsilon_1)(\alpha_2+\gamma_2)+4\tau_1\lambda_2\Big]+\tfrac{21}{20}\,c_{12}\,\beta_3^2\,\sigma_{11}\,\sigma_7\,\varrho_1^2\big[\rho_2(\alpha_2+\gamma_2)-\tfrac{\lambda_2(\mu_2+\delta_2)}{2}\big]\\
&\quad+a\,\beta_4\,\sigma_7\Big[(\alpha_1+\gamma_1-4\mu_1)(\alpha_2+\gamma_2)+(-\lambda_2-2\rho_2)\lambda_1+(\mu_2+\delta_2)(\alpha_1+\gamma_1)+4\rho_1\lambda_2\Big],\\
F_{33} &= 40\Big\{\beta_4\Big[-272\,c_{12}\,\beta_2\,\sigma_{11}\,\sigma_7\,\varrho_1^2\Big(\rho_2(\alpha_2+\gamma_2)-\frac{27\lambda_2(\mu_2+\frac{7\delta_2}{27})}{34}\Big)-240\,c_2\,\sigma_{11}\,\sigma_7\,(\alpha_2+\gamma_2)\Big]
\end{aligned}$$

$$+ 40\, a\, \beta_4\, \sigma_7 \Big[(\gamma_2 - 3\mu_2 + \alpha_2 + \delta_2)\alpha_1 + \alpha_2\gamma_1 + (\gamma_2 - 3\mu_2 + \delta_2)\gamma_1 - \lambda_1(\lambda_2 - 2\rho_2) \Big]$$

$$+ 80\, a\, \beta_4\, \sigma_{11} \Big[(\theta_2 - 3\tau_2)(\alpha_2 + \gamma_2) + 4\lambda_2\varepsilon_2 \Big] + 102\, c_{12}\, \beta_3^2\, \sigma_{11}\, \sigma_7\, \varrho_1^2 \Big[\rho_2(\alpha_2 + \gamma_2) - \tfrac{27\lambda_2(\mu_2 + \frac{7\delta_2}{27})}{34} \Big] \Big\},$$

$$F_4 = \rho_2(\alpha_2 + \gamma_2) - \tfrac{\lambda_2(\mu_2 + \delta_2)}{2},$$

$$F_{44} = \rho_2(\alpha_2 + \gamma_2) - \tfrac{3\lambda_2(\mu_2 - \frac{\delta_2}{3})}{2},$$

$$\beta = \beta_2\beta_4 - \tfrac{3\beta_3^2}{8}.$$

- $$\delta_1 = \frac{\sigma_{11}^2 \big(E_1\, \sigma_{12} + 2E_2\, \sigma_7\big) - \sigma_{11}\sigma_{12}\big(E_3\, \sigma_{12} + E_4\, \sigma_7\big) + \sigma_{12}^2\sigma_7 E_5}{\sigma_7\, \sigma_{12}\, \big[-\lambda_1\sigma_{12} + \sigma_{11}(\alpha_2 + \gamma_2) \big]}.$$

where

$$E_1 = 2(\theta_1 + \tau_1)\lambda_2 + 2(\tau_2 + \theta_2)(\alpha_2 + \gamma_2),$$

$$E_2 = \rho_2(\alpha_2 + \gamma_2) - \tfrac{1}{2}(\mu_2 + \delta_2)\lambda_2,$$

$$E_3 = 2\lambda_1(\tau_2 + \theta_2) + 2(\theta_1 + \tau_1)(\alpha_1 + \gamma_1),$$

$$E_4 = 2(\lambda_1\rho_2 - \rho_1\lambda_2) - (\alpha_1 + \gamma_1)(\mu_2 + \delta_2) + (\alpha_2 + \gamma_2)\mu_1,$$

$$E_5 = \lambda_1\mu_1 - 2\rho_1(\alpha_1 + \gamma_1).$$

- $$f_1 = \frac{X_7\, \sigma_{12}^4 + X_8\, \sigma_{12}^3 + X_9\, \sigma_{12}^2 + \Big(16\, X_1\, \sigma_{11}^3\, \sigma_7\, (\alpha_2 + \gamma_2)(\tau_2 + \theta_2) + 6\, X_1 X_2\, \sigma_{11}^2\, \sigma_7^2\Big)\sigma_{12} + 8\, X_1^2\, \sigma_{11}^3\, \sigma_7^2}{50\, \sigma_7^2\, \sigma_{12}^2\, \big(\sigma_{11}(\alpha_2 + \gamma_2) - \lambda_1\sigma_{12}\big)^2},$$

$$f_2 = \frac{8\, \lambda_1^2\, \sigma_{12}^4\, (\tau_2 + \theta_2)^2 + 50\, X_{10}\, \lambda_1\, \sigma_{12}^3 + X_{11}\, \sigma_{12}^2 + 50\, X_{12}\, \sigma_{11}\, \sigma_7\, \sigma_{12} + 8\, X_1^2\, \sigma_{11}^2\, \sigma_7^2}{50\, \sigma_7^2\, \sigma_{12}\, \big(\lambda_2\sigma_{11} - (\alpha_1 + \gamma_1)\sigma_{12}\big)^2}.$$

where

$$X_1 = \rho_2(\alpha_2 + \gamma_2) - \tfrac{\lambda_2}{2}(\mu_2 + \delta_2),$$

$$X_2 = (\alpha_1 + \gamma_1)(\alpha_2 + \gamma_2) - \lambda_1\Big(\lambda_2 + \tfrac{8\rho_2}{3}\Big) + \tfrac{4}{3}(\alpha_1 + \gamma_1)(\mu_2 + \delta_2),$$

$$X_3 = \tfrac{4}{3}(\alpha_1 + \gamma_1)(\mu_2 + \delta_2) - \lambda_1\Big(\lambda_2 + \tfrac{16\rho_2}{3}\Big),$$

$$X_4 = 2(\alpha_1 + \gamma_1)\gamma_2 + X_3,$$

$$X_5 = (\alpha_1 + \gamma_1)(\alpha_2^2 + \gamma_2^2) + \alpha_2 X_4 - \lambda_1\gamma_2\Big(\lambda_2 + \tfrac{16\rho_2}{3}\Big) + \tfrac{4}{3}\lambda_1\lambda_2(\mu_2 + \delta_2),$$

$$\begin{aligned} X_6 = \sigma_{11}&\Big[\lambda_1(100h_2\alpha_2 + 100h_2\gamma_2 - 50g_2\lambda_2) - 50g_2(\alpha_1 + \gamma_1)(\alpha_2 + \gamma_2)\Big] \\ &- 2\Big[(\alpha_1 + \gamma_1)(\alpha_2 + \gamma_2) + \lambda_1(-\lambda_2 + 4\rho_2) - 2(\alpha_1 + \gamma_1)(\mu_2 + \delta_2)\Big] \\ &\times \Big[(\alpha_1 + \gamma_1)(\alpha_2 + \gamma_2) + \lambda_1(-\lambda_2 - \rho_2) + \tfrac{1}{2}(\alpha_1 + \gamma_1)(\mu_2 + \delta_2)\Big], \end{aligned}$$

$$X_7 = 8\sigma_{11}\lambda_1^2(\tau_2 + \theta_2)^2 + 50\sigma_7^2(\alpha_1 + \gamma_1)(g_1\lambda_1 - h_1(\alpha_1 + \gamma_1)),$$

$$\begin{aligned} X_8 = &-16\, \lambda_1(\tau_2 + \theta_2)^2(\alpha_2 + \gamma_2)\, \sigma_{11}^2 \\ &- 50\, \sigma_7^2\sigma_{11}\Big[g_1(\alpha_1 + \gamma_1)(\alpha_2 + \gamma_2) + \lambda_2\big(g_1\lambda_1 - 2h_1(\alpha_1 + \gamma_1)\big)\Big] \\ &- 6\, (\tau_2 + \theta_2)\, \lambda_1\, X_2\, \sigma_7\, \sigma_{11}, \end{aligned}$$

$$X_9 = 8(\tau_2 + \theta_2)^2(\alpha_2 + \gamma_2)^2\sigma_{11}^3 + 50\sigma_7\sigma_{11}^2\Big[\lambda_2\sigma_7(g_1(\alpha_2 + \gamma_2) - h_1\lambda_2) + \tfrac{3}{25}(\tau_2 + \theta_2)X_5\Big]$$

$$
\begin{aligned}
&-2\sigma_7^2\Big[(\alpha_1+\gamma_1)(\alpha_2+\gamma_2)+\lambda_1(-\lambda_2+4\rho_2)-2(\alpha_1+\gamma_1)(\mu_2+\delta_2)\Big]\\
&\times\Big[(\alpha_1+\gamma_1)(\alpha_2+\gamma_2)+\lambda_1(-\lambda_2-\rho_2)+\tfrac{1}{2}(\alpha_1+\gamma_1)(\mu_2+\delta_2)\Big],
\end{aligned}
$$

$$X_{10}=\sigma_7^2\big[g_2(\alpha_1+\gamma_1)-\lambda_1 h_2\big]-\tfrac{3}{25}(\tau_2+\theta_2)X_2\sigma_7-\tfrac{8}{25}(\tau_2+\theta_2)^2(\alpha_2+\gamma_2)\sigma_{11},$$

$$X_{11}=\sigma_7^2X_6+6\sigma_{11}\sigma_7X_5(\tau_2+\theta_2)+8\sigma_{11}^2(\tau_2+\theta_2)^2(\alpha_2+\gamma_2)^2,$$

$$X_{12}=\sigma_7\Big[\sigma_{11}(\alpha_2+\gamma_2)(g_2\lambda_2-h_2(\alpha_2+\gamma_2))+\tfrac{3}{25}X_1X_2\Big]+\tfrac{8}{25}(\tau_2+\theta_2)(\alpha_2+\gamma_2)\sigma_{11}X_1.$$

- $\kappa=\sqrt{\dfrac{2\left[\left(\frac{3\beta_3^2}{8}-\beta_2\beta_4\right)c_{12}\varrho_1^2\sigma_{12}-a\beta_4\right]}{c_{12}\sigma_{12}\beta_4}}.$
- $\omega=\dfrac{18432\,\lambda_1\varrho_1^4c_{12}^2\sigma_{12}^4(\tau_2+\theta_2)Z_1+4608\,\varrho_1^4c_{12}^2\sigma_{12}^3Z_5-\sigma_{12}^2Z_6-128\,a^2\beta_4^2\sigma_{12}Z_7-128\,\sigma_7a^2\sigma_{11}\beta_4^2Z_2}{1536\,\sigma_{12}\beta_4^2c_{12}\big(\lambda_1\sigma_{12}^2(\tau_2+\theta_2)-\sigma_{12}Z_7-\sigma_7\sigma_{11}Z_2\big)}.$

where

$$
\begin{aligned}
Z_1&=\beta_0\beta_4^3-\left(\frac{\beta_1\beta_3}{4}+\frac{\beta_2^2}{144}\right)\beta_4^2+\frac{13}{192}\beta_2\beta_3^2\beta_4-\frac{13}{1024}\beta_3^4,\\
Z_2&=\rho_2(\alpha_2+\gamma_2)-\frac{\lambda_2}{2}(\mu_2+\delta_2),\\
Z_3&=\sigma_7\Big[(\alpha_1+\gamma_1)(\alpha_2+\gamma_2-\tfrac{13}{4}(\mu_2+\delta_2))-\lambda_1\lambda_2+\tfrac{13}{2}\lambda_1\rho_2\Big]\\
&\quad-\tfrac{13}{2}\sigma_{11}(\alpha_2+\gamma_2)(\tau_2+\theta_2),\\
Z_4&=(\alpha_1+\gamma_1)\big(\alpha_2+\gamma_2-2(\mu_2+\delta_2)\big)-\lambda_1\lambda_2+4\lambda_1\rho_2,\\
Z_5&=\beta_4^2\Bigg\{\beta_0\beta_4\Big[Z_4\,\sigma_7-4\,\sigma_{11}(\alpha_2+\gamma_2)(\tau_2+\theta_2)\Big]\\
&\qquad+\sigma_7\Big[\frac{\beta_2^2}{36}\Big((\alpha_1+\gamma_1)(\alpha_2+\gamma_2+\tfrac{1}{2}(\mu_2+\delta_2))-(\lambda_2+\rho_2)\lambda_1\Big)-\frac{\beta_1\beta_3}{4}Z_4\Big]\\
&\qquad+\sigma_{11}(\alpha_2+\gamma_2)(\tau_2+\theta_2)\Big(\beta_1\beta_3+\frac{\beta_2^2}{36}\Big)\Bigg\}+Z_3\left(\frac{\beta_3^2\beta_2}{24}\beta_4-\frac{\beta_3^4}{128}\right),\\
Z_6&=\sigma_7Z_2\varrho_1^4c_{12}^2\sigma_{11}\Big[18432\,\beta_0\beta_4^3-4608\,\beta_4^2\Big(\beta_1\beta_3+\frac{\beta_2^2}{36}\Big)+1248\,\beta_2\beta_3^2\beta_4-234\,\beta_3^4\Big]-128\,\beta_4^2a^2\lambda_1(\tau_2+\theta_2),\\
Z_7&=\sigma_7\Big[(\alpha_1+\gamma_1)\Big(\alpha_2+\gamma_2+\tfrac{1}{2}(\mu_2+\delta_2)\Big)-\lambda_1(\lambda_2+\rho_2)\Big]+\sigma_{11}(\alpha_2+\gamma_2)(\tau_2+\theta_2).
\end{aligned}
$$

ORCID

Rajveer Singhay, https://orcid.org/0009-0009-9938-2064; **Sachin Kumar**, https://orcid.org/0000-0001-6883-7788; **Mohamed E. M. Alngar**, https://orcid.org/0000-0002-5436-7268; **Reham M. A. Shohib**, https://orcid.org/0000-0001-8352-5491; **Lina S. Calucag**, https://orcid.org/0000-0002-9090-3283; **Anjan Biswas**, https://orcid.org/0000-0002-8131-6044

REFERENCES

[1] A. Ankiewicz, and N. Akhmediev, "Higher-order integrable evolution equation and its soliton solutions," Phys. Lett. A, **378**, 358–361 (2014). https://doi.org/10.1016/j.physleta.2013.11.031

[2] A. Ankiewicz, Y. Wang, S. Wabnitz, and N. Akhmediev, "Extended nonlinear Schrödinger equation with higher-order odd and even terms and its rogue wave solutions," Phys. Rev. E, **89**, 012907 (2014). https://doi.org/10.1103/physreve.89.012907

[3] N. Karjanto, "Modeling wave packet dynamics and exploring applications: a comprehensive guide to the nonlinear Schrödinger equation," Mathematics, **12**(5), 744 (2024). https://doi.org/10.3390/math12050744

[4] A. R. Seadawy, and B. Alsaedi, "Contraction of variational principle and optical soliton solutions for two models of nonlinear Schrödinger equation with polynomial law nonlinearity," AIMS Mathematics, **9**(3), 6336–6367 (2024). https://doi.org/10.3934/math.2024309

[5] C. Peng, Z. Li, and H. Zhao, "New exact solutions to the Lakshmanan–Porsezian–Daniel equation with Kerr law of nonlinearity," Mathematical Problems in Engineering, **2022**(1), 7340373 (2022). https://doi.org/10.1155/2022/7340373

[6] H. H. Hussein, H. M. Ahmed, and W. Alexan, "Analytical soliton solutions for cubic–quartic perturbations of the Lakshmanan–Porsezian–Daniel equation using the modified extended tanh function method," Ain Shams Engineering Journal, **15**(3), 102513 (2024). https://doi.org/10.1016/j.asej.2023.102513

[7] N. A. Kudryashov, "Painlevé analysis of the Sasa–Satsuma equation," Phys. Lett. A, **525**, 129900 (2024). https://doi.org/10.1016/j.physleta.2024.129900

[8] P. Li, S. Shi, C. Xu, and M. U. Rahman, "Bifurcations, chaotic behavior, sensitivity analysis and new optical solitons solutions of Sasa–Satsuma equation," Nonlinear Dynamics, **112**(9), 7405–7415 (2024). https://doi.org/10.1007/s11071-024-09438-6

[9] A. Chowdury, D. J. Kedziora, A. Ankiewicz, and N. Akhmediev, "Soliton solutions of an integrable nonlinear Schrödinger equation with quintic terms," Phys. Rev. E, **91**, 032922 (2015). https://doi.org/10.1103/physreve.90.032922

[10] A. Chowdury, D. J. Kedziora, A. Ankiewicz, and N. Akhmediev, "Breather-to-soliton conversions described by the quintic equation of the nonlinear Schrödinger hierarchy," Phys. Rev. E, **91**, 032928 (2015). https://doi.org/10.1103/physreve.91.032928

[11] A. Chowdury, D. J. Kedziora, A. Ankiewicz, and N. Akhmediev, "Breather solutions of the integrable quintic nonlinear Schrödinger equation and their interactions," Phys. Rev. E, **91**, 022919 (2015). https://doi.org/10.1103/physreve.91.022919

[12] A. Biswas, J. Vega-Guzman, Y. Yıldırım, L. Moraru, C. Iticescu, and A. A. Alghamdi, "Optical solitons for the concatenation model with differential group delay: undetermined coefficients," Mathematics, **11**(9), 2012 (2023). https://doi.org/10.3390/math11092012

[13] A. H. Arnous, A. Biswas, Y. Yildirim, and A. S. Alshomrani, "Optical solitons for the dispersive concatenation model with differential group delay," Nonlinear Optics, Quantum Optics: Concepts in Modern Optics, **61** (2025).

[14] R. Singh, and S. Kumar, "Lie symmetry analysis, closed-form solutions and dynamics for the kinetics of phase separation in iron (Fe–Cr–X (X = Mo, Cu)) based on ternary alloys," Nonlinear Dynamics, **112**, 20255–20267 (2024). https://doi.org/10.1007/s11071-024-10112-0

[15] P. J. Olver, *Applications of Lie Groups to Differential Equations*, 2nd edn., Graduate Texts in Mathematics, vol. 107, (Springer, New York, NY, 1993).

ОПТИЧНІ СОЛІТОНИ ДЛЯ МОДЕЛІ КОНКАТЕНАЦІЇ З ДИФЕРЕНЦІАЛЬНОЮ ГРУПОВОЮ ЗАТРИМКОЮ, ПОБУДОВАНІ НА ОСНОВІ СИМЕТРІЇ ЛІ ТА ПІДХОДУ КУМАРА-МАЛІКА

Раджвір Сінгхай[1], Сачін Кумар[1], Мохамед Е. М. Алнгар[2], Рехам М. А. Шохіб[3], Ліна С. Калукаг[4], Анджан Бісвас[5,6,7,8,9*]

[1]*Кафедра математики та статистики, Центральний університет Пенджабу, Батінда, 151401, Пенджаб, Індія*
[2]*Програма математичної освіти, Факультет освіти та мистецтв, Університет Сохар, Сохар 311, Оман*
[3]*Кафедра фундаментальних наук, Факультет економіки та бізнес-адміністрування, Інноваційний університет, Шаркія, Єгипет*
[4]*Кафедра математики та природничих наук, Технологічний університет Бахрейну, Королівство Бахрейн*
[5]*Кафедра математики та фізики, Державний університет Грамблінга, Грамблінг, Луїзіана–71245, США*
[6]*Кафедра математики, Факультет природничих наук, Технічний університет Караденіз, Трабзон—61080, Туреччина*
[7]*Кафедра фізики та електроніки, Університет Хазар, Баку, Аризона—1096, Азербайджан*
[8]*Кафедра математики та прикладної математики, Університет медичних наук Сефако Макгатхо, Медунса—0204, Преторія, Південна Африка*
[9]*Науково-дослідний центр прикладних наук, Приватний університет прикладних наук, Амман—11937, Йорданія*

У цій роботі розглядається узагальнена модель конкатенації для двопроменевих оптичних волокон та отримані нові точні солітонні розв'язки. Використовуючи аналіз симетрії Лі, зв'язані еволюційні рівняння перетворюються через відповідні змінні подібності в керовану систему звичайних диференціальних рівнянь. Отримана редукована система потім обробляється методом Кумара-Маліка для отримання кількох класів явних розв'язків, записаних еліптичними, яскравими солітонними, темними солітонними та тригонометричними розв'язками Якобі. З відповідними обмеженнями параметрів ці класи спрощуються до знайомих яскравих, темних та періодичних солітонних хвиль. Для ілюстрації фізичної поведінки отриманих структур представлені репрезентативні графіки, які підкреслюють їхні особливості поширення та якісну стабільність. Загалом, поєднання редукції симетрії зі схемою Кумара-Маліка розширює каталог аналітичних розв'язків для моделі конкатенації та поглиблює розуміння нелінійної динаміки імпульсів у двопроменевих середовищах.

Ключові слова: *структура конкатенації; аналіз симетрії групи Лі; метод Кумара-Маліка; оптичні солітонні хвилі; двопроменеві волоконні середовища; розв'язки еліптичної функції Якобі*